FLIGHT LOAD INVESTIGATION OF HELICOPTER EXTERNAL LOADS

Horace T. Hone

United Aircraft Corporation

Prepared for:

Army Air Mobility Research and Development Laboratory

February 1975

EUSTIS DIRECTORATE POSITION STATEMENT

Flight reaction loads obtained from instrumented flights of external cargo payloads have been reduced to flight load design factors pertinent to helicopter cargo attachment hard points, sling systems, and external cargo attachment interface strength design.

The flight load factors derived by this program collaborate data developed by a previous flight load factor investigation using a computer-simulated flight program. The load factor design curves in USAAMRDL Technical Report 72-36, "Design Guide for Load Suspension Points, Slings, and Aircraft Hard Points", can be used with confidence to design structurally adequate helicopter external cargo transport systems for all flight dynamics contingencies.

This report has been reviewed by this Directorate and is considered to be technically sound. The contractual technical monitor for this program was Steven Hola, Military Operations Technology Division.

Unclassified

SECURITY CLASSIFICATION OF THIS PAGE (When Data Entered)

REPORT DOCUMENTATION PAGE		READ INSTRUCTIONS BEFORE COMPLETING FORM
1. REPORT NUMBER USAAMRDL-TR-74-104	2. GOVT ACCESSION NO.	3. RECIPIENT'S CATALOG NUMBER AD-A008 394
4. TITLE (and Subtitle) FLIGHT LOAD INVESTIGATION OF HELICOPTER EXTERNAL LOADS		5. TYPE OF REPORT & PERIOD COVERED Final Report 6. PERFORMING ORG. REPORT NUMBER SER-50906
7. AUTHOR(s) Horace T. Hone		8. CONTRACT OR GRANT NUMBER(s) DAAJ02-74-C-0016
9. PERFORMING ORGANIZATION NAME AND ADDRESS Sikorsky Aircraft Division of United Aircraft Corporation Stratford, Connecticut 06602		10. PROGRAM ELEMENT, PROJECT, TASK AREA & WORK UNIT NUMBERS Project 1F262203AH86
11. CONTROLLING OFFICE NAME AND ADDRESS Eustis Directorate U.S. Army Air Mobility Research and Development Laboratory, Fort Eustis, Virginia 23604		12. REPORT DATE February 1975 13. NUMBER OF PAGES 74
14. MONITORING AGENCY NAME & ADDRESS(if different from Controlling Office)		15. SECURITY CLASS. (of this report) Unclassified 15a. DECLASSIFICATION/DOWNGRADING SCHEDULE

16. DISTRIBUTION STATEMENT (of this Report)

Approved for public release; distribution unlimited.

17. DISTRIBUTION STATEMENT (of the abstract entered in Block 20, if different from Report)

18. SUPPLEMENTARY NOTES

19. KEY WORDS (Continue on reverse side if necessary and identify by block number)

Helicopter - External Load Combination
Helicopter Flight Loads
Helicopter Load Factors
CH-54 Helicopter
Sling Dynamic Strength Criteria

20. ABSTRACT (Continue on reverse side if necessary and identify by block number)

Any cargo that is freely suspended from a helicopter fuselage, by any of several available methods, does not experience the same dynamic loads as the aircraft. For various reasons the load factors may be amplified and peak out of phase with those of the helicopter. This has long been suspected as a major contribution to premature failures in slings, pendants, and attachment points at the aircraft or cargo. A theoretical analysis of the load factor relationship duri.. various flight maneuvers was conducted by Sikorsky Aircraft

DD FORM 1 JAN 73 1473

Unclassified

SECURITY CLASSIFICATION OF THIS PAGE (When Data Entered)

BLOCK 20. ABSTRACT (Continued)

in 1971 by means of a hybrid computer simulation of the coupled motion of a CH-54 helicopter and several types of external loads, conducted in real time and nonreal time on a fixed-base and a moving-base simulator. Actual flight tests have now been performed on a CH-54 helicopter to investigate the validity of that part of the simulator program from which was derived the relationship between helicopter load factor and sling tension load factor. The results show agreement with the conclusions of the analysis except for the somewhat special case of four-point suspension, which produced load factors about 15% higher than the simulator study predicted.

PREFACE

This work is related to the following previous efforts:

USAAMRDL Task 1F162203A43501 (Contract DAAJ02-70-C-0021)

USAAMRDL House Task AS70-11

USAAMRDL Task 1F162203AA33 (Contract DAAJ02-71-C-0016)

USAAMRDL Task 1F163209DB3303 (Contract DAAJ02-72-C-0008)

Reference to the reports generated by the above tasks is made in the text of this report.

TABLE OF CONTENTS

LIST OF ILLUSTRATIONS

LIST OF TABLES

INTRODUCTION

PROGRAM OBJECTIVE

The purpose of this task was to check by flight test measurements the results from a previous simulator study of the forces produced in slings and associated hard points during the carriage of slung loads on helicopters, thereby establishing a confidence level for the strength criteria derived from the simulator study.

BACKGROUND

This work may be regarded as the fifth in a series of investigations resulting from a conference sponsored by the U.S. Army in 1968 to explore phenomena associated with the carriage of externally suspended loads on helicopters, and to establish more reliable strength requirement data for the load slings and for their interfaces at the helicopter and at the load. The previous investigations were "Criteria for Externally Suspended Helicopter Loads,"[1] "Effect of Helicopter External Loads on Sling Properties,"[2] "Design Guide for Load Suspension Points, Slings and Aircraft Hard Points,"[3] and "Development of Cargo Slings With Nondestructive Checkout Systems."[4] The first three were part of a program undertaken by the Eustis Directorate as an immediate consequence of the meeting. This fifth investigation constitutes an experimental sequel to the first, which was the simulator study. A brief description of the latter is therefore presented in the next section.

---

1. Briczinski, S.J., and Karas, G.R., CRITERIA FOR EXTERNALLY SUSPENDED HELICOPTER LOADS, Sikorsky Aircraft, Division of United Aircraft Corporation; USAAMRDL Technical Report 71-61, Eustis Directorate, U.S. Army Air Mobility Research and Development Laboratory, Fort Eustis, Virginia, November 1971, AD 740072.

2. Gustafson, Arthur J., Jr., Bryan, Max E., McIlwean, Edgar H., and Birocco, Eugene A., EFFECTS OF HELICOPTER EXTERNAL LOADS ON SLING PROPERTIES; USAAMRDL Technical Report 73-91, Eustis Directorate, U.S. Army Air Mobility Research and Development Laboratory, Fort Eustis, Virginia, September 1973, AD 774267.

3. Huebner, Walter E., DESIGN GUIDE FOR LOAD SUSPENSION POINTS, SLINGS, AND AIRCRAFT HARD POINTS, Sikorsky Aircraft, Division of United Aircraft Corporation; USAAMRDL Technical Report 72-36, Eustis Directorate, U.S. Army Air Mobility Research and Development Laboratory, Fort Eustis, Virginia, July 1972, AD 747814.

4. Hone, Horace T., Huebner, Walter E., and Baxter, Donald J., DEVELOPMENT OF CARGO SLINGS WITH NONDESTRUCTIVE CHECKOUT SYSTEMS, Sikorsky Aircraft, Division of United Aircraft Corporation; USAAMRDL Technical Report 73-106, Eustis Directorate, U.S. Army Air Mobility Research and Development Laboratory, Fort Eustis, Virginia, February 1974, AD 777497.

TERMINOLOGY

To facilitate cross-reference with the simulator study report (Reference 1), similar terms and symbols have been used where possible for components and parameters in this report.

Figures 1, 2, 3 and 4 show typical sling arrangements and define the major parts. The items labelled "leg" are sometimes termed "nylon leg" in Reference 1, but this nomenclature has been discarded since steel cables were used for the flight tests. The word "cable" has been retained to denote the single wire-rope of the main hoist or any one of the four load leveller cables. The word "pendant" is sometimes used in Reference 1 to denote the single wire-rope of the main hoist, and although this term has been discarded, the suffix "P" has been used in the same manner as on page 59 of Reference 1. The word "bridle" is sometimes used in Reference 1 to denote a three-legged or a four-legged assembly, and although this term has been discarded, the suffix "B" has been used in the same manner as on page 59 of Reference 1.

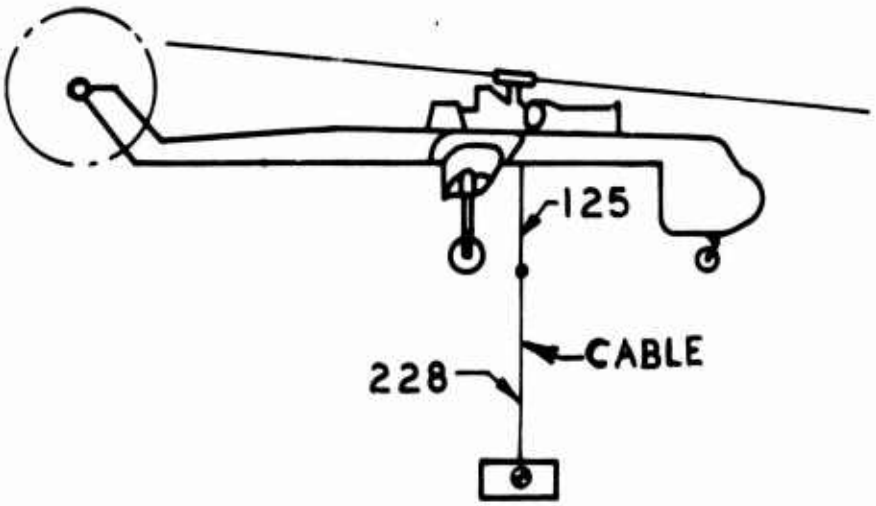

(Note: Dimensions in inches unless otherwise noted)

Figure 1. Single-Legged Sling Suspension of a 15,000-Pound Solid Concrete Block.

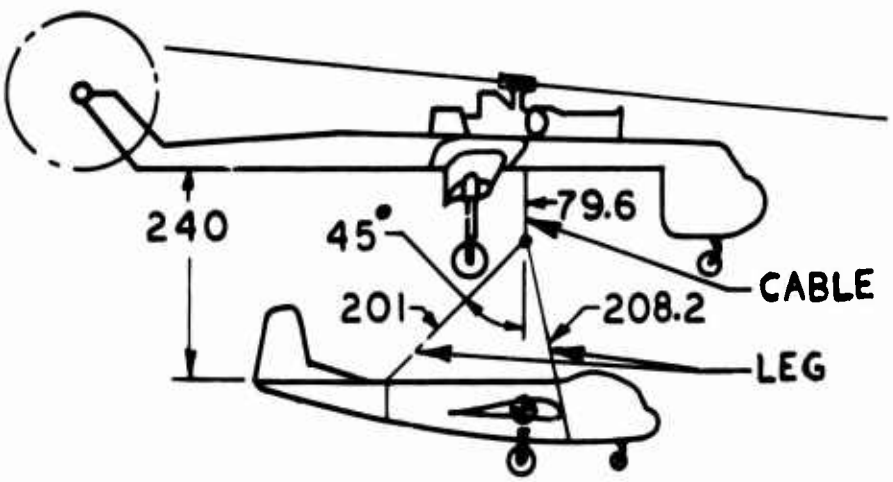

TRUE SLING LEG
ANGLE 12°5′

(Note: Dimensions in inches unless otherwise noted)

Figure 2. Three-Legged Bridle Suspension of a 12,000-Pound Fixed-Wing Aircraft.

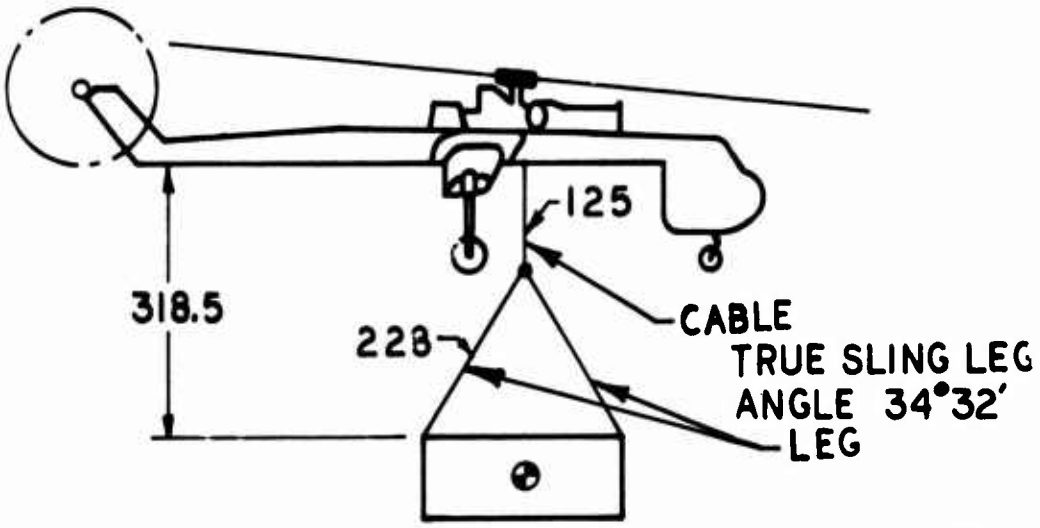

(Note: Dimensions in inches unless otherwise noted)

Figure 3. Single-Point Suspension of 8-Foot x 8-Foot x 20-Foot Container From a Four-Legged Sling.

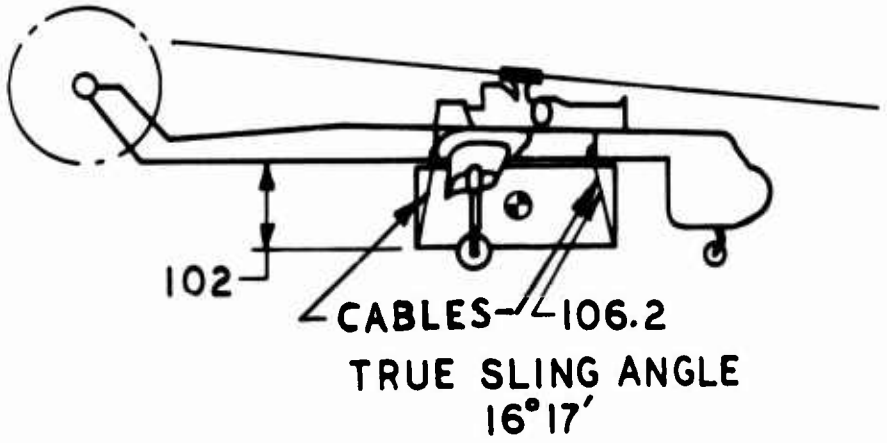

(Note: Dimensions in inches unless otherwise noted)

Figure 4. Multipoint Suspension of 8-Foot x 8-Foot x 20-Foot Container.

SIMULATOR STUDY SUMMARY

PARAMETERS

The hybrid simulator system (described later) determined the various forces and load factors (listed below) generated during various flight maneuvers (listed below) when various load types (listed below) are carried externally by various suspension methods (listed below) from a CH-54 helicopter. To perform actual flight investigations covering all possible combinations of the variables listed would be impracticable. Those selected for flight test will be detailed later (see page 15).

Forces and Load Factors

Table 1 summarizes the principal forces and load factors which were derived from the simulator program. The force values (Columns 1 and 2) were divided by the static trim force values (Column 3) to convert them to non-dimensional load factor forms (Columns 2 and 3). The symbols are those used in Reference 1.

TABLE 1.- LIST OF FORCES AND LOAD FACTORS

Description		Instantaneous Force (Pounds) Column 1	Maximum Dynamic Force (Pounds) Column 2	Static Trim Force (Pounds) Column 3	Instantaneous Load Factor Column 4	Maximum Dynamic Load Factor Column 5
Helicopter, Vertical		—	—	--	N_z	$N_{z_{max}}$
Cable Tension		T_i	$T_{C_{max}}$	T_{C_S}	LFT_C	$LFT_{C_{max}}$
Leg Tension		T_j	$T_{L_{max}}$	T_{L_S}	LFT_L	$LFT_{L_{max}}$
Helicopter Hard Point Force	Vertical	V_i	$V_{H_{max}}$	V_{H_S}	LFV_H	$LFV_{H_{max}}$
	Drag	D_i	$D_{H_{max}}$	D_{H_S}	LFD_H	$LFD_{H_{max}}$
	Side	S_i	$S_{H_{max}}$	S_{H_S}	LFS_H	$LFS_{H_{max}}$
	In-Plane	P_i	$P_{H_{max}}$	P_{H_S}	LFP_H	$LFP_{H_{max}}$
Load Hard Point Force	Vertical	V_k	$V_{L_{max}}$	V_{L_S}	LFV_L	$LFV_{L_{max}}$
	Drag	D_k	$D_{L_{max}}$	D_{L_S}	LFD_L	$LFD_{L_{max}}$
	Side	S_k	$S_{L_{max}}$	S_{L_S}	LFS_L	$LFS_{L_{max}}$
	In-Plane	P_k	$P_{L_{max}}$	P_{L_S}	LFP_L	$LFP_{L_{max}}$

(In addition, to facilitate the analysis, certain other forces were derived: e.g., T_i was resolved along helicopter and load axes; T_j was assigned a component due to external forces; T_{C_S}, T_{L_S}, V_{H_S} and V_{L_S} were subdivided into front and rear; etc.)

Flight Maneuvers

The following flight maneuvers were simulated:

Vertical takeoff
Symmetrical dive and pullout
Roll reversal
Yaw reversal in hover; pedal kick
Approach to hover
Longitudinal stick stroke in hover
Lateral stick stroke in hover
Rolling pullout

(In addition, the effect of gusts was input at certain points in the program.)

Load Types

The following load types were analyzed (a load being categorized according to the ratio of weight, in pounds, to maximum frontal area, in square feet, which the load might be expected to present to the line of flight).

Type I - high density (ratio more than 250)
Type II - medium density (ratio between 250 and 50)
Type III - low density (ratio less than 50)

(In addition, a Type IV was created to include loads which have inherent aerodynamic characteristics, e.g., aircraft, helicopter, fuselages, etc.)

Suspension Methods

The following suspension methods were analyzed. They are illustrated in Figures 1, 2, 3 and 4, respectively.

Single point with single cable.
Single point with single cable and three legs.
Single point with single cable and four legs.
Four points with four cables.

(In addition, the special case of a Brooks and Perkins pallet suspended from four points on twelve cables and the effect of one leg breaking in configurations having four legs were analyzed.)

DESCRIPTION OF SIMULATOR SYSTEM

Fixed Base - Real Time

For each combination of suspension method, load type and maneuver, the various forces generated in the cables and at the hard points were derived by a PDP-6 computer solution of the coupled equations of motion for the CH-54 and the slung load, using the General Helicopter Simulation Program interfaced with a slung load simulation program. Both programs were developed by Sikorsky; the first simulates continuous flight of a single-rotor helicopter, and the second describes the motion of an external load. Control inputs were generated by a pilot in an S61 cockpit simulator and transmitted via an analog-digital converter to the computer. The computer solution to the motion equations was then returned via a digital-analog converter to the S61 cockpit simulator and displayed to the pilot on a Norden Contact Analog display system. The pilot control responses were then retransmitted to the computer, and the cycle was repeated throughout the maneuver. The system was therefore operating in real-time. There had to be at least 16 passes per second through the entire solution in real-time; otherwise the pilot could detect discrete changes being supplied to the display and would react unrealistically. This rate provided insufficient time for a thorough analytic solution of the helicopter/external load equations. The solution in real-time was therefore simplified and abbreviated, e.g., by using a rotor simulation consisting of only two blades and four segments per blade.

Fixed Base - Nonreal Time

A more thorough solution (for six blades, five segments) in nonreal-time was then run using the pilot inputs recorded from the real-time run to recreate the maneuvers on the computer. Thus, the only data retained from the the real-time runs were the pilot responses, and these replaced the simulator in nonreal-time (at a factor of X5). Also, the only data retained from the nonreal-time runs were the maximum nondimensionalized forces found within a given narrow aircraft load factor band, for each maneuver. A separate data monitor and acquisition program were set up to carry out the necessary scanning and filtering process; otherwise the quantity of data generated by 16 simulated passes per second would have been unmanageable.

Moving Base - Real Time

The real-time runs with "fixed-base", i.e., with the S61 cockpit simulator in static mode, were followed by real-time runs with "moving-base", i.e., with the S61 cockpit simulator in dynamic mode. Thus the computer fed motion cues as well as visual cues to the pilot, correctly orienting the cockpit throughout each maneuver. It was therefore possible to evaluate the effect on pilot reaction of superimposing physical data. It should be mentioned also that the fixed-base runs were restricted to the first three maneuvers listed previously, namely, vertical takeoff, symmetrical dive and pullout, and roll reversal; but the moving-base runs included all eight maneuvers, the additional ones being considered likely to cause pilot-induced oscillations.

Moving Base - Nonreal Time

As in the case of the fixed-base runs, the moving-base runs were repeated in nonreal time (at a factor of X5) to permit a more thorough analytical solution of the motion equations.

CONCLUSIONS FROM SIMULATOR STUDY

The main conclusions, as far as they are relevant to the flight investigation, were as follows:

1. Sling and hard-point load factors could sometimes be more than twice the helicopter load factor, thus exceeding its design criteria.

2. Symmetrical dive and pullout was usually the most critical maneuver.

3. There is often a gross maldistribution of forces on load hard points.

4. The density of a load is a significant parameter.

5. High load factors in sling and hard points are not necessarily associated with maneuvers which generate high load factors.

6. Sling geometry (leg or cable inclination) is an important parameter in determining maximum sling and hard point forces.

FLIGHT INVESTIGATION SUMMARY

PARAMETERS

Forces and Load Factors

Table 1 listed the principal forces and load factors derived from the simulator program. The only forces and load factors that were measured in the flight tests were: cable tension (T_i), leg tension (T_j), helicopter vertical (N_z), plus helicopter longitudinal and lateral (which were not involved in the simulator study, but may be denoted by the symbols N_x and N_y respectively). It will be evident that if the configuration geometry can be established, from a knowledge of hard point positions and tension member lengths, the hard point parameters listed in Table I could be resolved. These forces will be proportional to the tension in the appropriate cable or leg; hence the only requirement of the flight test is to determine maximum tensions ($T_{C_{max}}$ and $T_{L_{max}}$) and to associate them with the maximum helicopter vertical load factors ($N_{Z_{max}}$). The helicopter load factors were measured in three axes, but only the vertical (N_z) was considered to be significant, the longitudinal (N_x) and lateral (N_y) being recorded for contingency reasons. Cable and leg tensions (T_i and T_j) can be nondimensionalized into load factor forms (LFT_C and LFT_L) by calculation, since the static trim values (T_{C_S} and T_{L_S}) can be determined from a consideration of load weight and configuration geometry. This will be explained in more detail later (see page 34).

Flight Maneuvers

The same flight maneuvers as programmed on the fixed base simulation were flown; namely, vertical takeoff, symmetrical dive and pullout, and roll reversal. The symmetrical dive and pullout was sometimes performed as a levelling-out from a dive at approximately 1,000 ft/min. Roll reversal could be defined as "yaw kick" in the case of the flights with the concrete block and "rolling turn" in the case of the flights with containers, these being the most practical load-inducing maneuvers.

Load Types

The loads were of Type I, II and III, i.e., high, medium and low density, represented by a solid concrete block, a loaded container, and an empty container respectively. They are described in more detail in the next section.

Suspension Methods

The suspension methods were as illustrated in Figures 1, 3 and 4; i.e., single point with single cable (used with the concrete block), single point with single cable and four legs (used with the loaded and empty containers), and four points with four cables (used with the loaded and empty containers). A spreader bar was used when the container was suspended from the top as in Figure 3.

TEST AIRCRAFT

The aircraft used in the flight tests was a CH54 (S/N 69-18462) loaned by the U.S. Army. The only modification required (apart from the installation of the instrumentation described below) was the fitting of a slip ring above the main cargo swivel hook to transmit load signals from the load cells to the aircraft when carrying loads on single point as in Figures 1 and 3. The slip ring used was a type W102-100 made by Wendon Company Inc.

TEST LOADS

Type I

This was a rectangular concrete block with a lifting eye set in the center of the top face. It weighed 15,000 pounds.

Type II

This was a MILVAN version of the standard 8-foot x 8-foot x 20-foot container, loaded with concrete blocks, which were strapped to the floor structure. It weighed 14,876 pounds.

Type III

This was a MILVAN version of the standard 8-foot x 8-foot x 20-foot container, unloaded. It weighed 1,195 pounds.

TEST INSTRUMENTATION

Internal

Internal instrumentation consisted of an oscillograph for recording aircraft load factors and cable tensions, and three accelerometers mounted orthogonally near the aircraft center of gravity for measuring load factors in vertical, longitudinal and lateral directions.

The accelerometers had a calibration sensitivity of 1.33G, 1.37G and 1.70G respectively.

External

External instrumentation consisted of a 50,000-pound load cell (used as shown in Figures 5, 6, and 8) for measuring the tension in the aircraft main hoist cable, and four 10,000-pound load cells (used as shown in Figures 6, 7, 8, and 9) for measuring the tensions in the four sling legs or four load-leveller cables.

Calibration data for the load cells is recorded in Tables 2, 3, 4, 5 and 6.

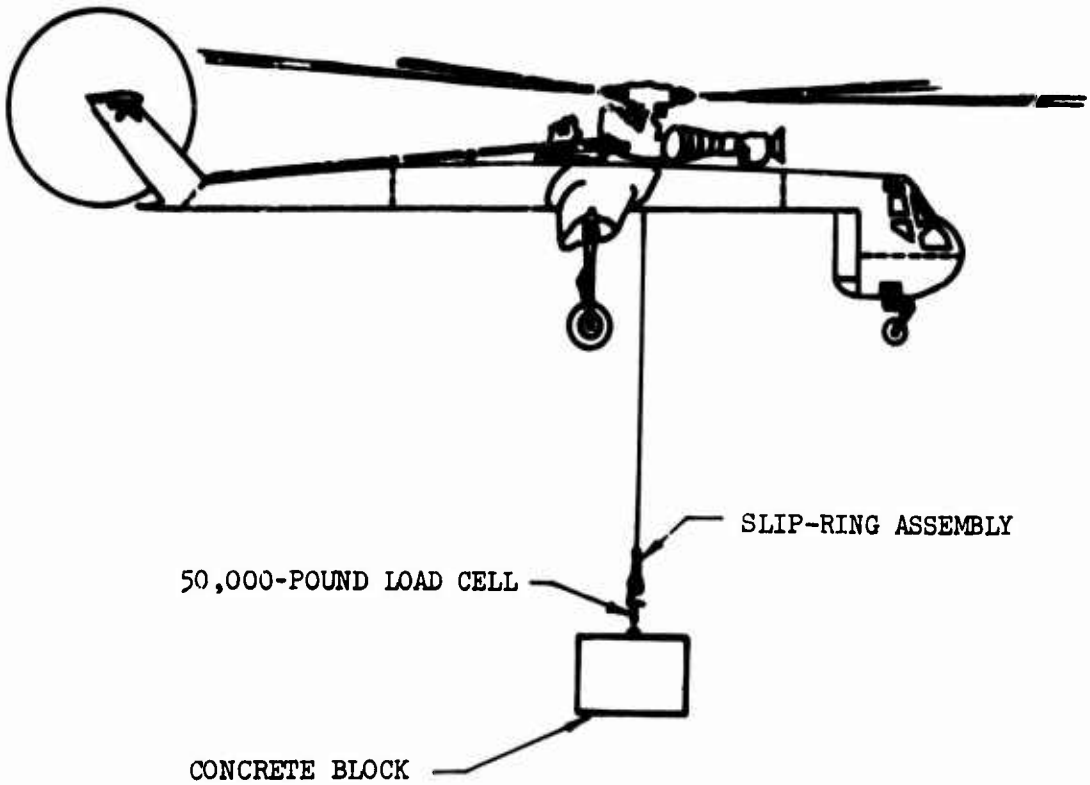

Figure 5. Configuration IP.

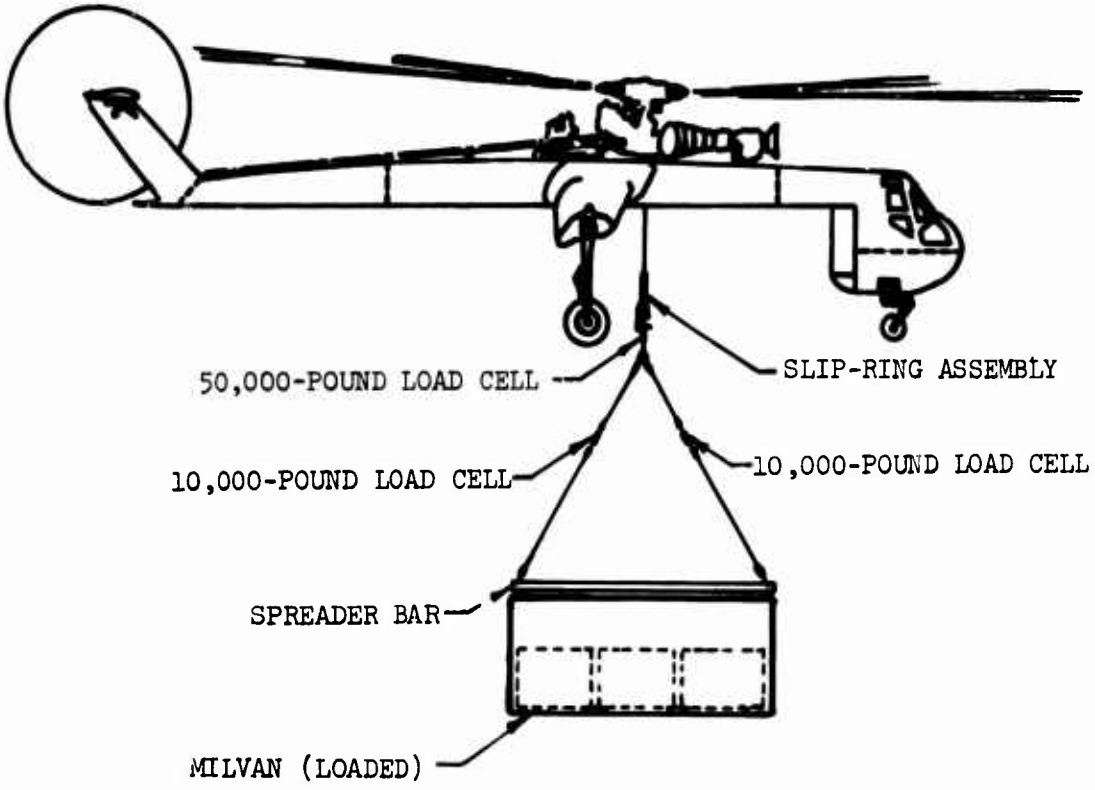

Figure 6. Configuration IIB.

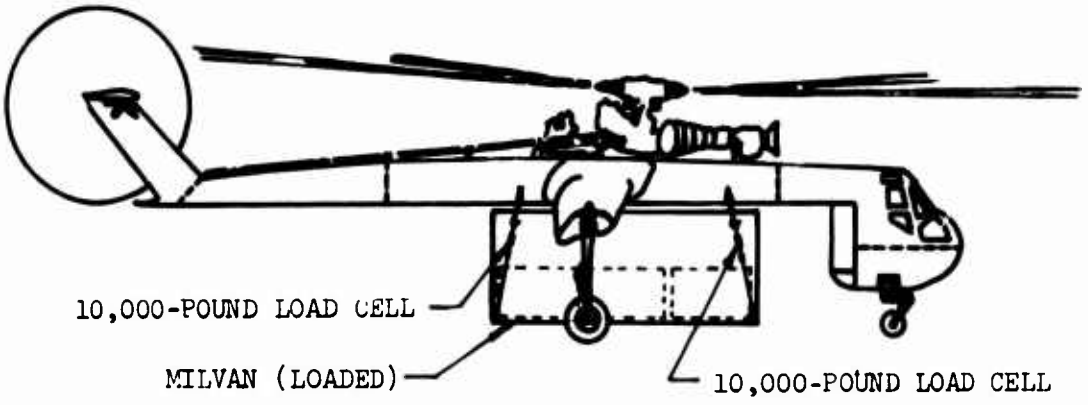

Figure 7. Configuration II 4PT.

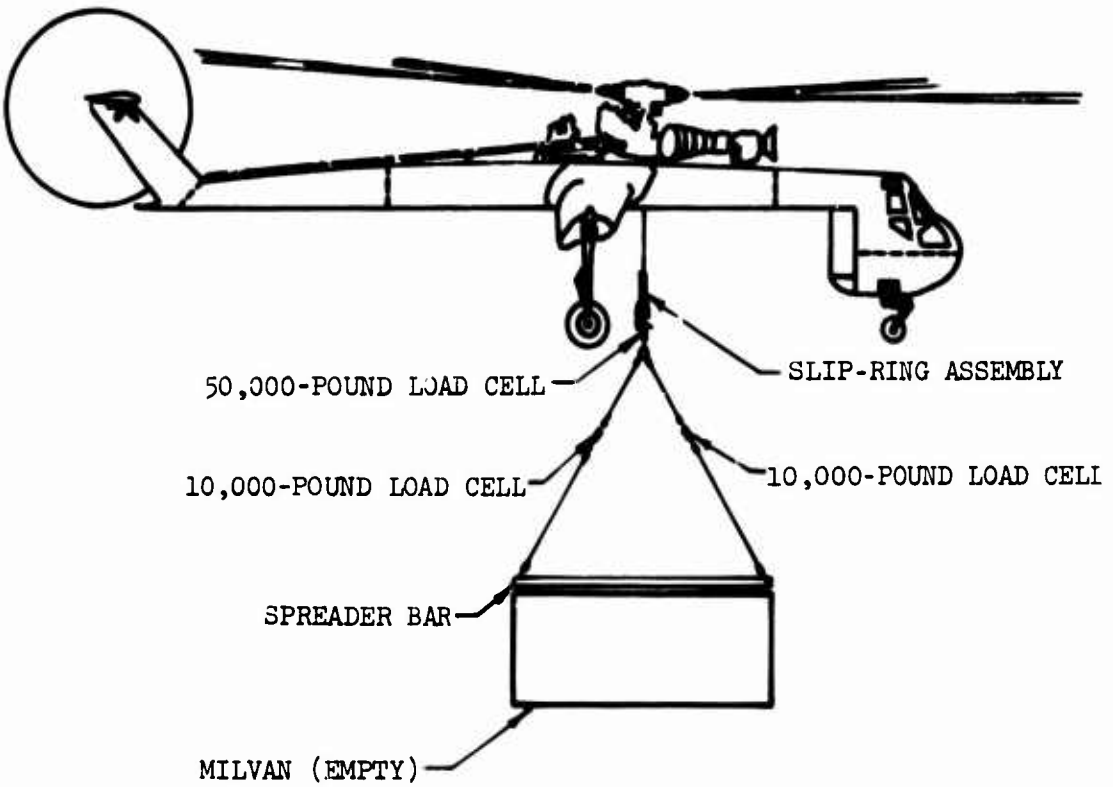

Figure 8. Configuration IIIB.

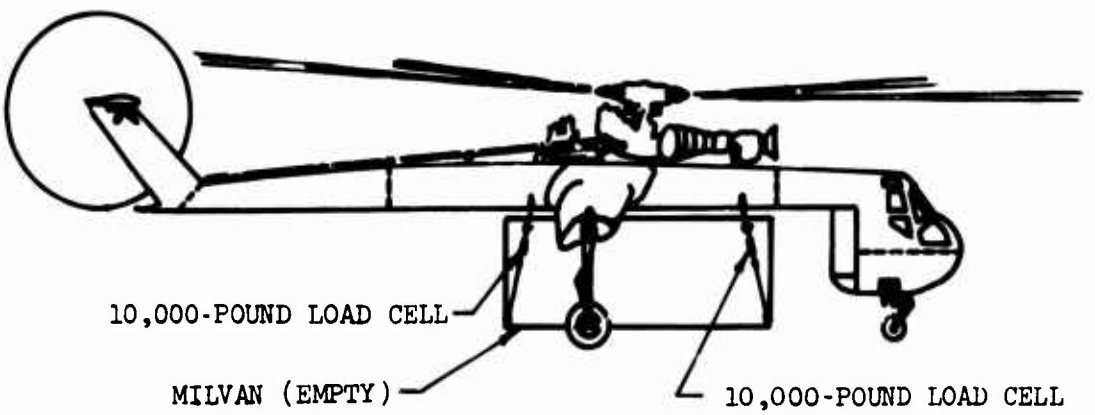

Figure 9. Configuration III 4PT.

TABLE 2. LOAD CELL CALIBRATION, 50,000 LB, NO. N-970

Applied Load (lb/1000)	Reading Inverted (micro-in./in.)
0	0
5	- 396
10	- 791
15	-1,188
20	-1,584
25	-1,980
30	-2,379
35	-2,778
40	-3,177
45	-3,576
50	-3,976
45	-3,576
40	-3,177
35	-2,777
30	-2,379
25	-1,981
20	-1,583
15	-1,187
10	- 790
5	- 395
0	0

TABLE 3. LOAD CELL CALIBRATION, 10,000 LB, NO. 96957		
Applied Load (lb/1000)	Reading	
	Erect (micro-in./in.)	Inverted (micro-in./in.)
0	0	0
1	- 599	+ 596
2	-1,196	+1,192
3	-1,791	+1,787
4	-2,394	+2,384
5	-2,988	+2,980
6	-3,588	+3,578
7	-4,188	+4,175
8	-4,789	+4,771
9	-5,384	+5,368
10	-5,983	+5,964
9	-5,388	+5,368
8	-4,787	+4,771
7	-4,188	+4,174
6	-3,589	+3,579
5	-2,991	+2,981
4	-2,392	+2,385
3	-1,793	+1,786
2	-1,195	+1,190
1	- 599	+ 594
0	0	0

TABLE 4. LOAD CELL CALIBRATION, 10,000 LB, NO. 96961

Applied Load (lb/1000)	Reading	
	Erect (micro-in./in.)	Inverted (micro-in./in.)
0	0	0
1	- 600	+ 595
2	-1,201	+1,191
3	-1,800	+1,787
4	-2,401	+2,384
5	-3,000	+2,980
6	-3,602	+3,577
7	-4,200	+4,175
8	-4,800	+4,772
9	-5,401	+5,370
10	-6,001	+5,965
9	-5,403	+5,369
8	-4,801	+4,772
7	-4,201	+4,175
6	-3,600	+3,577
5	-3,000	+2,980
4	-2,402	+2,383
3	-1,799	+1,785
2	-1,199	+1,189
1	- 599	+ 592
0	0	0

TABLE 5. LOAD CELL CALIBRATION, 10,000 LB, 96986		
Applied Load lb/1000	Reading	
	Erect (micro-in./in.)	Inverted (micro-in./in.)
0	0	0
1	- 598	+ 599
2	-1,195	+1,193
3	-1,791	+1,791
4	-2,390	+2,385
5	-2,986	+2,983
6	-3,583	+3,578
7	-4,181	+4,176
8	-4,777	+4,775
9	-5,375	+5,369
10	-5,970	+5,967
9	-5,374	+5,371
8	-4,775	+4,774
7	-4,176	+4,197
6	-3,578	+3,578
5	-2,980	+2,983
4	-2,385	+2,386
3	-1,789	+1,788
2	-1,193	+1,193
1	- 595	+ 597
0	0	0

TABLE 6. LOAD CELL CALIBRATION, 10,000 LB, NO. 97026

Applied Load (lb/1000)	Reading	
	Erect (micro-in./in.)	Inverted (micro-in./in.)
0	0	0
1	- 597	+ 597
2	-1,193	+1,195
3	-1,789	+1,787
4	-2,386	+2,384
5	-2,982	+2,978
6	-3,579	+3,576
7	-4,178	+4,173
8	-4,777	+4,773
9	-5,373	+5,366
10	-5,968	+5,962
9	-5,373	+5,370
8	-4,776	+4,771
7	-4,179	+4,172
6	-3,581	+3,577
5	-2,985	+2,982
4	-2,390	+2,385
3	-1,790	+1,790
2	-1,196	+1,193
1	- 600	+ 599
0	0	0

TEST HARDWARE

Special sets of 6 x 19 IWRC stainless steel wire rope assemblies were fabricated in order to simulate the geometry of the configuration of Figures 1, 3 and 4, and to incorporate the load cells previously described. The cables were depicted in Figures 5, 6, 7, 8 and 9 together with the associated attachment shackles and eyebolts. The latter were threaded to fit the load cells and to provide for length adjustment in the components of the four-point configurations.

TEST PROGRAM

The flight load investigation was completed during six test flights listed in Table 7. It will be noted that the flights were not performed in the same order in which the various configurations were listed in Reference 1 and in the previous sections of this report. To minimize confusion, the flight test results in the next section are referenced by configuration (in the order IP, IIB, II 4PT, IIIB, III 4PT) rather than flight number.

TABLE 7. TEST FLIGHT CONFIGURATIONS

Flight No.	Type	Load Description	Suspension Method		Configuration Type
			Points	Tension Members	
1	I	Concrete Block	Single	Single Cable	IP
2 & 3	III	Empty MILVAN	Four	Four Cable	III 4PT
4	II	Loaded MILVAN	Four	Four Cable	II 4PT
5	III	Empty MILVAN	Single	Single Cable, Four Leg	IIIB
6	II	Loaded MILVAN	Single	Single Cable, Four Leg	IIB

For each configuration, the three subject maneuvers - vertical takeoff, symmetrical dive and pullout, and roll reversal - were performed at least six times. On each occasion the pilot endeavored to achieve the maximum vertical acceleration within the aircraft's capability.

FLIGHT TEST RESULTS

OSCILLOGRAPH RECORDS

On each flight the oscillograph was recording throughout every maneuver. A typical section of an oscillograph trace is reproduced in Figures 10, 11, 12 and 13. This was taken from Vertical Takeoff No. 1 for Flight No. 6 (Configuration IIB). At the top is a 100 c/s time base. Under this is a calibration datum line followed by the longitudinal, lateral and vertical aircraft accelerometer traces. The first two reveal the effects of rotor vibration but vary only slightly in general level. The vertical trace contains the only significant flight load factor information. Since this was a "B" (Bridle) configuration, there are five load cell traces, the first one being generated by the 50,000-pound load cell in the aircraft main hoist cable and the remainder by the 10,000-pound load cell in each of the four legs, respectively, for the aft left, aft right, forward left, and forward right positions. The main load cell trace is above the vertical accelerometer trace.

OSCILLOGRAPH DATA REDUCTION

The 4 or 5 seconds of trace generated during each performance of each maneuver were examined to determine the peak values of cable or leg tensions and the associated peak value of aircraft load factor. These were measured and tabulated for each performance of each of the three subject maneuvers.

In many instances a series of peaks occurred; therefore, the peaks following the primary peaks were measured and tabulated, for although their absolute values may be lower, the ratio of tension load factor to aircraft load factor may be higher for the secondary set of values. (The purpose of the investigation is to determine maximum effect-to-cause relationships rather than maximum effects and causes.)

The vertical accelerometer trace did not necessarily peak concurrently with the load cell traces. This was not unexpected, but it was not difficult to correlate the peaks.

To clarify the method of interpretation of the oscillograph data, the trace reproduced on Figures 10 through 13 is represented in a more graphic form on Figure 14. The time scale has been condensed by a factor of approximately 3, and a numerical scale of K pounds has been assigned to the ordinates. The redundant longitudinal and lateral accelerometer traces have been omitted as they are irrelevant. A consolidated trace representing the sum of the four leg load cells has been added for reference purposes The values of first peaks and second peaks have been identified. Figures 15 and 16 are similarly scaled representations of the traces taken from Symmetrical Dive and Pullout No. 2 and No. 4 for the same flight.

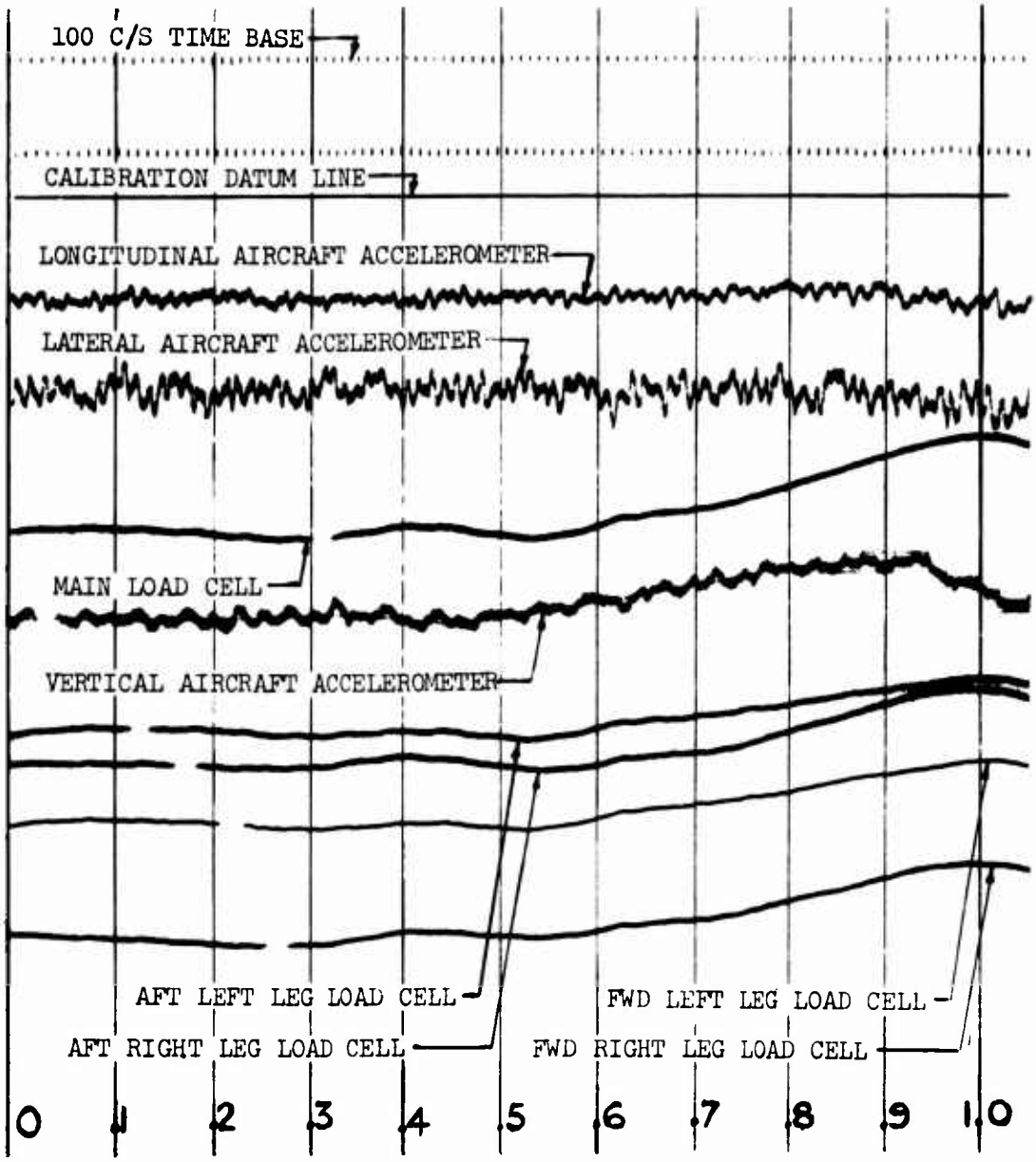

Figure 10. Oscillograph Trace, Configuration IIB, VTO No. 1, 0-1.0 Second.

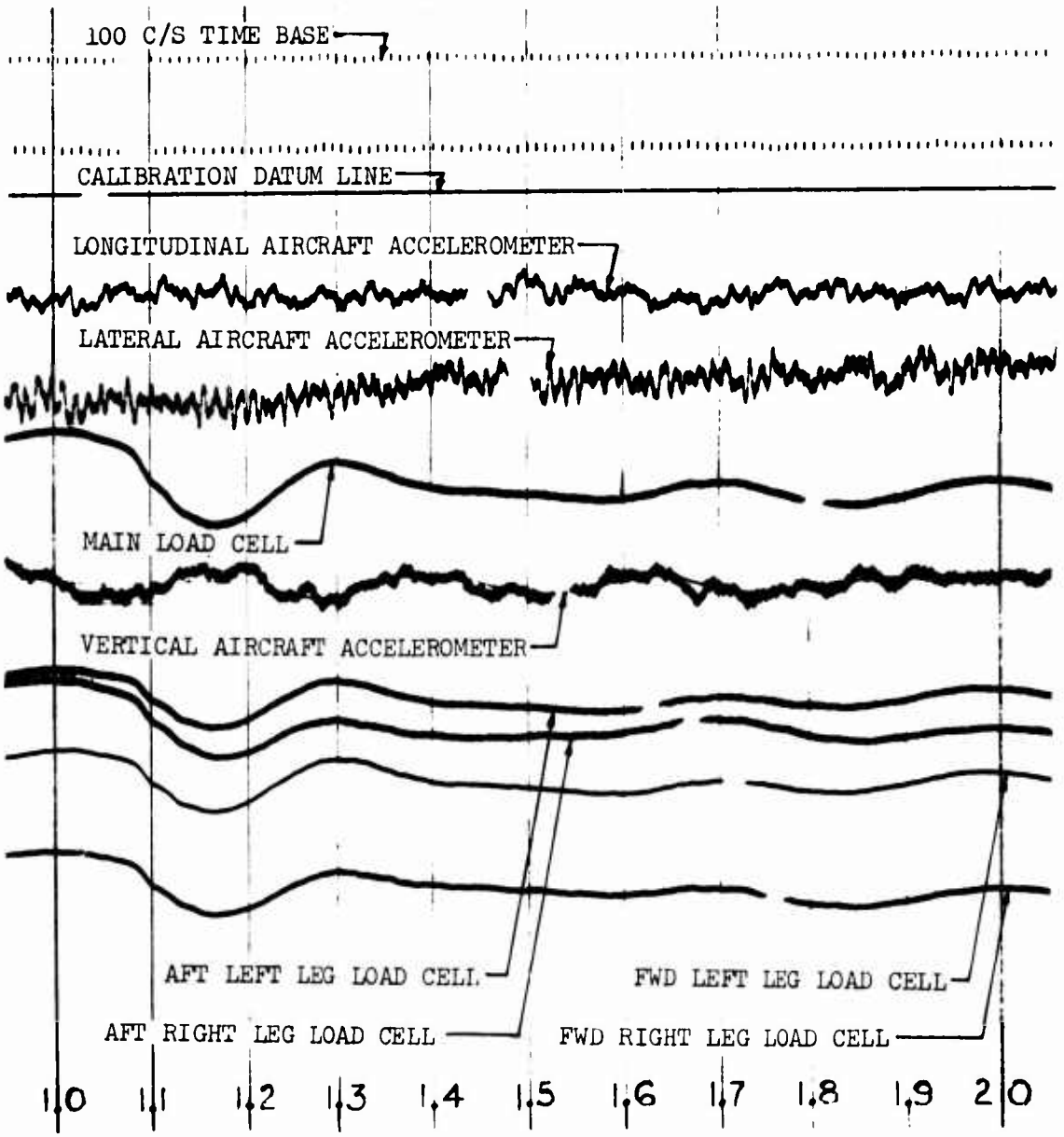

Figure 11. Oscillograph Trace, Configuration IIB, VTO No. 1, 1.0-2.0 Seconds.

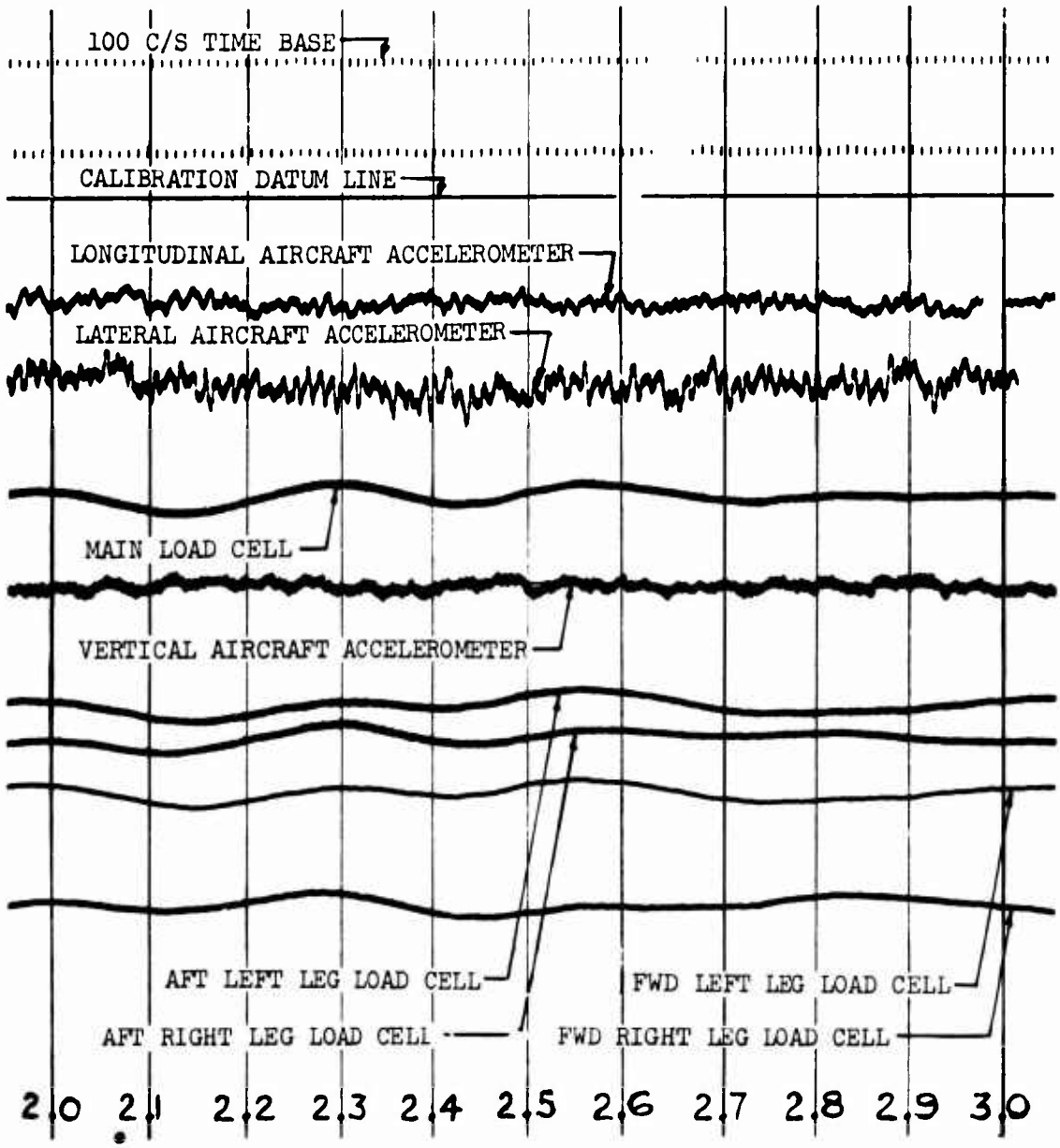

Figure 12. Oscillograph Trace, Configuration IIB, VTO, No. 1, 2.0-3.0 Seconds

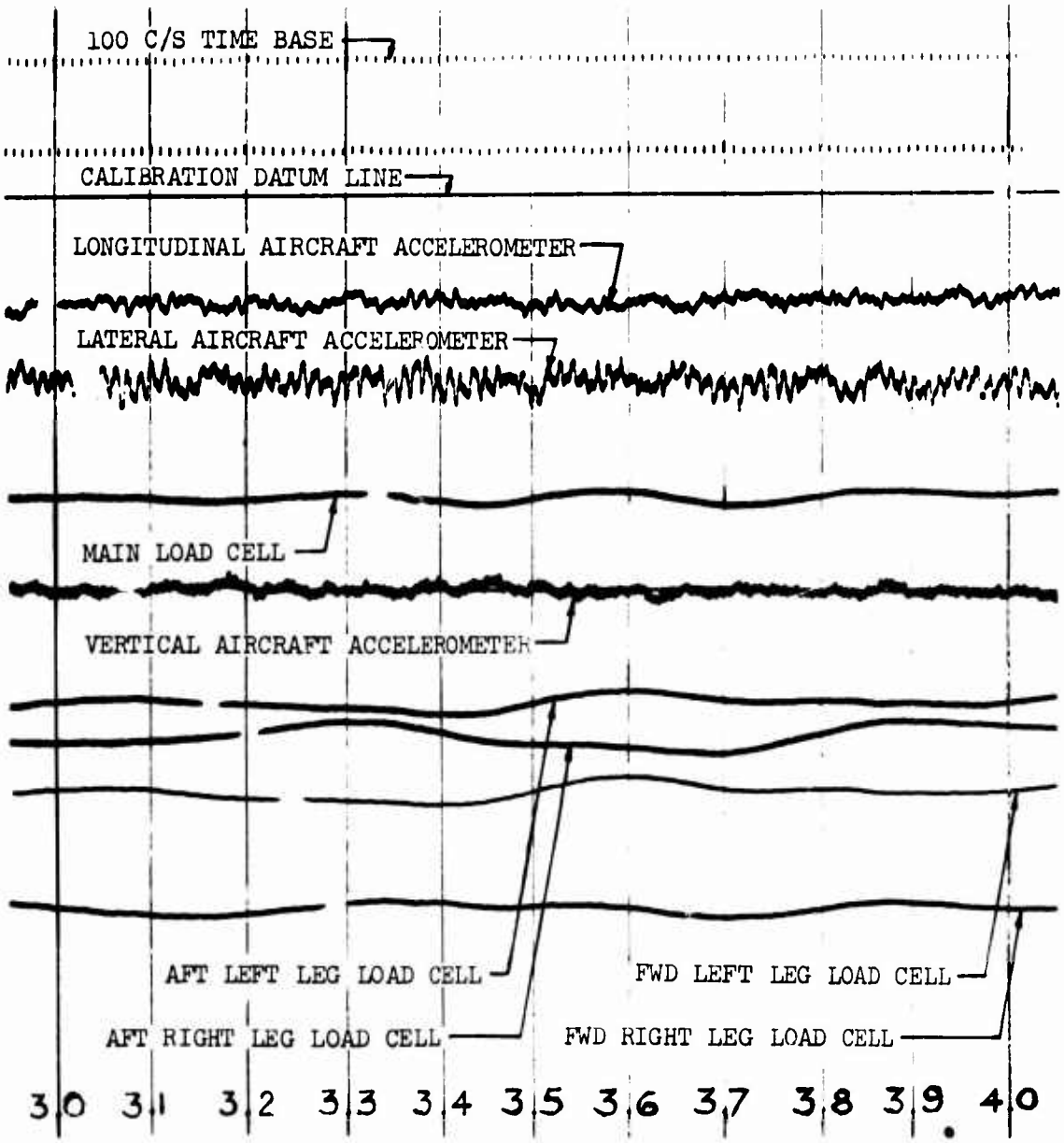

Figure 13. Oscillograph Trace, Configuration IIB, VTO, No. 1, 3.0-4.0 Seconds.

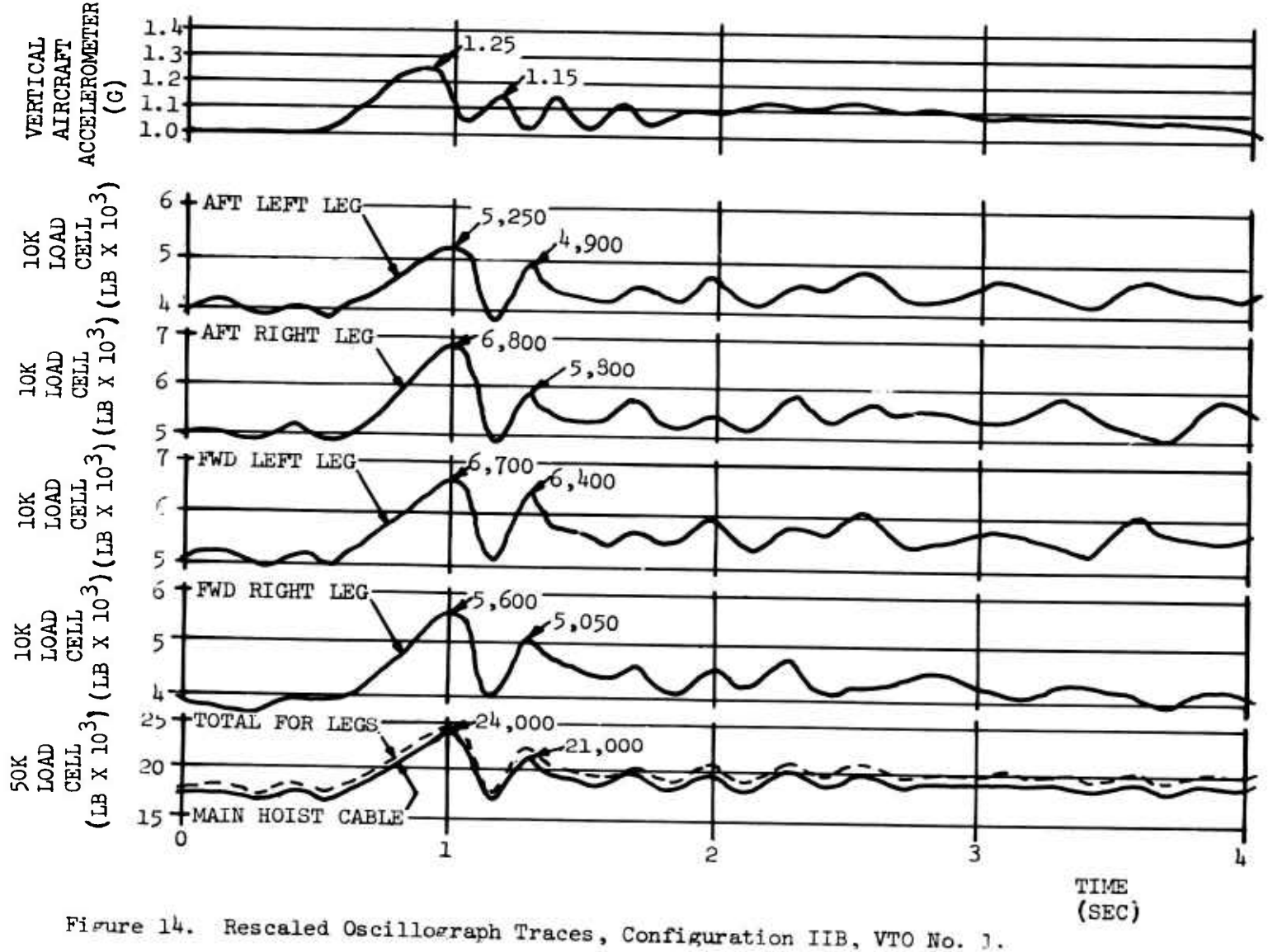

Figure 14. Rescaled Oscillograph Traces, Configuration IIB, VTO No. 3.

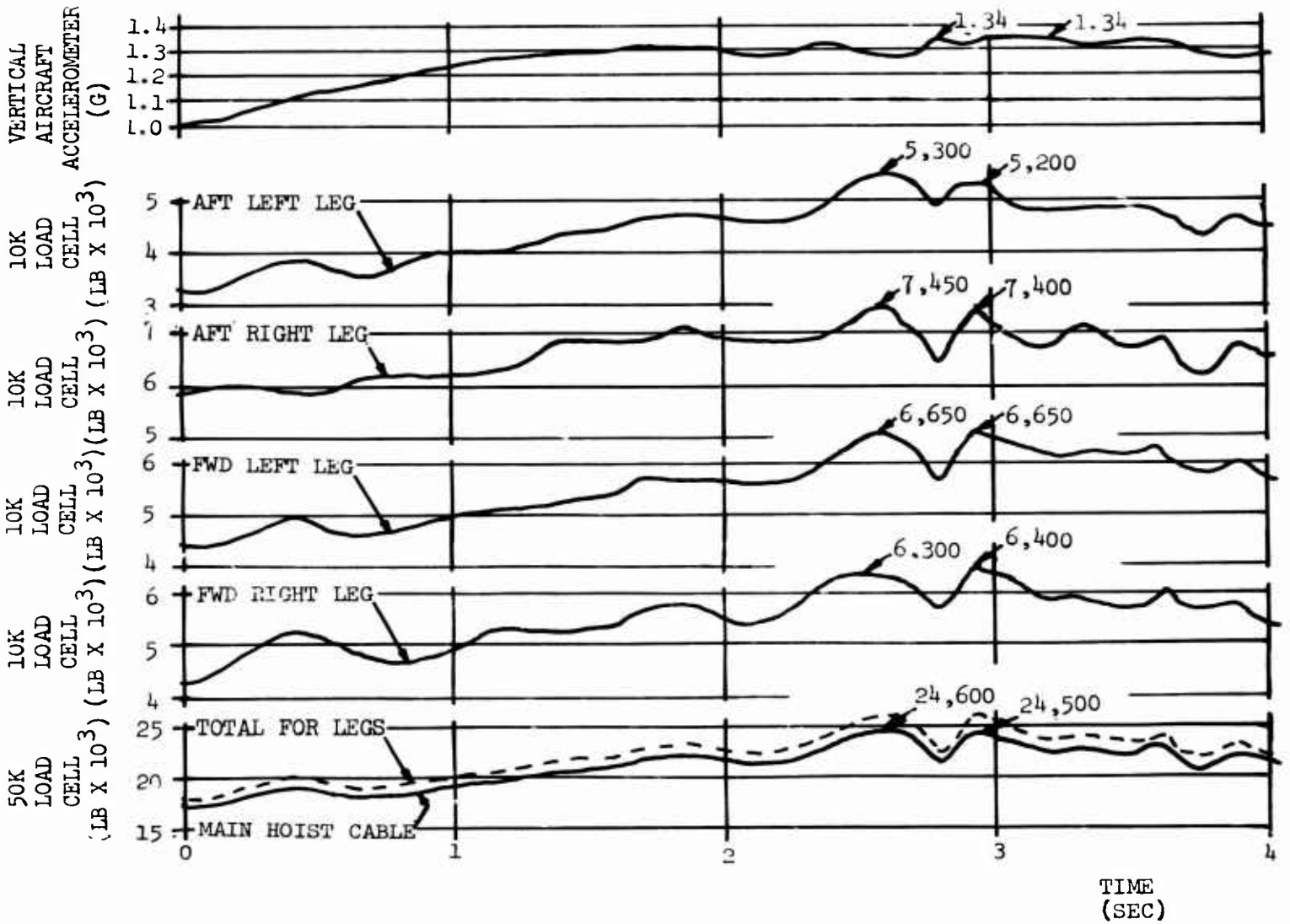

Figure 15. Rescaled Oscillograph Traces, Configuration IIB, SDPO No. 2.

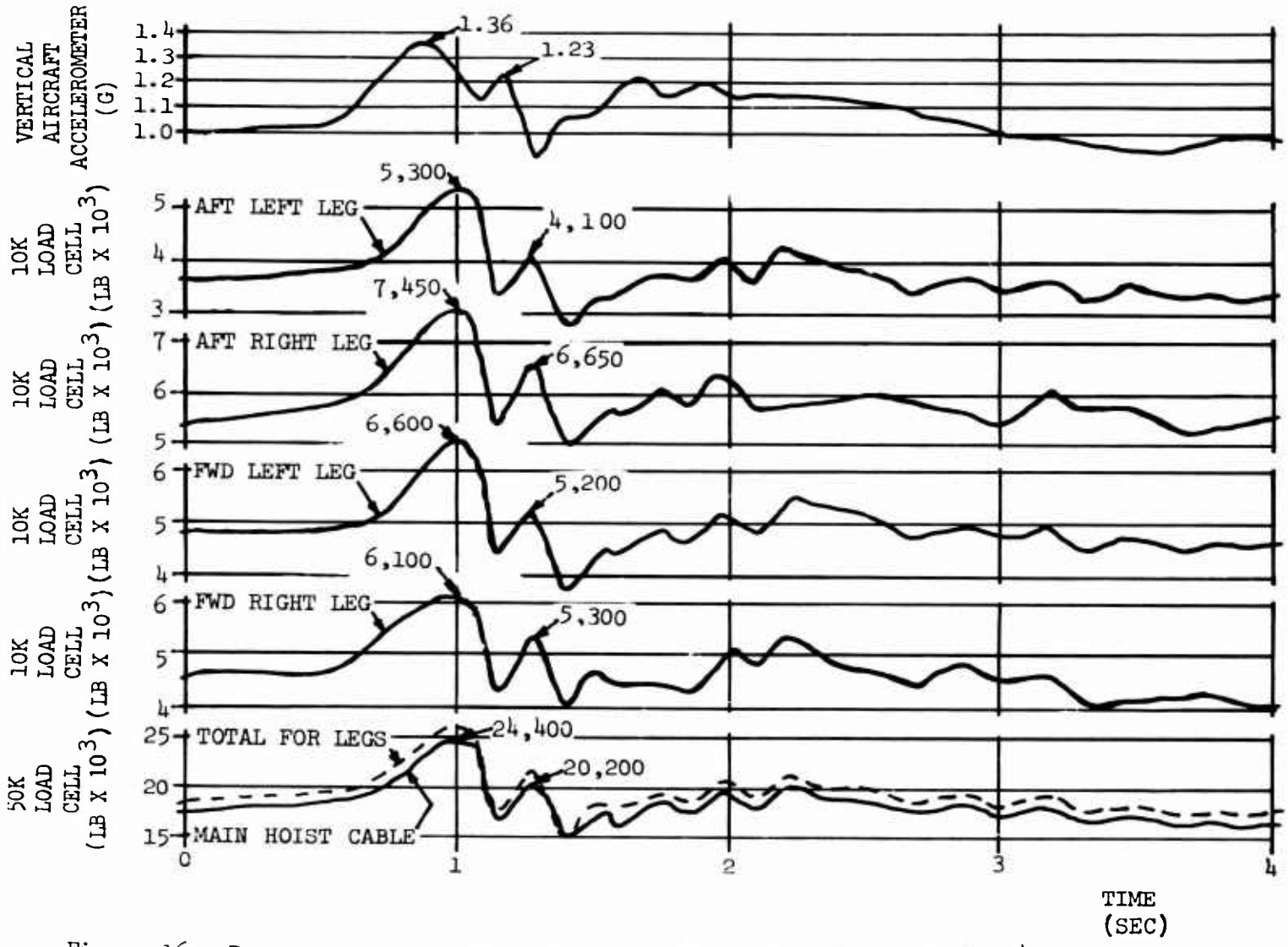

Figure 16. Rescaled Oscillograph Traces. Configuration IIB, SDPO No. 4.

DATA TABULATION

Tables 8 through 12 record the data applicable to Configurations IP, IIB, II 4PT, IIIB and III 4PT respectively. The maneuver and peak numbers (where applicable) are indicated. Referring to the sample trace graphs in Figures 14, 15 and 16, the peak values annotated thereon will be seen in Table 9 against VTO No. 1, SDPO No. 2 and SDPO No. 4, respectively.

For reference purposes, the tables also record the longitudinal and lateral accelerometer maximums, the trace values when the helicopter was in a state of steady hover, and (for Configurations II 4PT and III 4PT) the sum of the four cable load cells. For Configurations IIB and IIIB, the identification of the legs as Forward Left, etc., is arbitrary, since the load spins in flight; these were purely for reference, but each leg retained its assigned identity throughout the tests.

DATA NONDIMENSIONALIZATION

The load cell force values listed in Tables 8 through 12 were converted to load factors in Tables 13 through 17 by applying the relevant divisors as explained below.

For Configuration IP the maximum main hoist cable readings were divided by the static weight of the concrete block, i.e., 15,000 pounds.

For Configuration IIB the maximum main hoist cable readings were divided by the static weight of the loaded container plus spreader bar, i.e., 15,838 pounds, and the maximum individual leg readings were divided by the static tension in each leg. The latter value was derived by calculating the true angle of a leg to the vertical and resolving the static weight of the loaded container plus spreader bar, i.e., 15,838 pounds, along four such legs. From the geometry of the configuration, the leg angle was found to be 36° 42', so the static tension in each of the four legs becomes 15,838/4 sec 36° 42', i.e., 4,938 pounds.

For Configuration II 4PT the maximum individual load leveller cable readings were divided by the static tension in each cable. The latter value was derived by calculating the true angle of a cable to the vertical and resolving the static weight of the loaded container, i.e., 14,876 pounds, along four such cables. From the geometry of the configuration, the cable angle was found to be 16° 16', so the static tension in each of the four cables becomes 14,876/4 sec 16° 16', i.e., 3,874 pounds.

For Configuration IIIB the maximum main hoist cable readings were divided by the static weight of the empty container plus spreader bar, i.e., 5,582 pounds, and the maximum individual leg readings were divided by the static tension in each leg. The latter value was derived by calculating the true angle of a leg to the vertical and resolving the static weight of the empty container plus spreader bar, i.e., 5,582 pounds, along four such legs. From the geometry of the configuration, the leg angle was found to be 36° 42', so the static tension in each of the four legs becomes 5,582/4 sec 36° 42', i.e., 1,741 pounds.

TABLE 8. PEAK VALUES, CONFIGURATION IP

Maneuver and Number		Aircraft Load Factor						Cable Tension	
		Longtdnl $N_{x_{max}}$		Lateral $N_{y_{max}}$		Vertical $N_{z_{max}}$		$T_{C_{max}}$	
		1st (G)	2nd (G)	1st (G)	2nd (G)	1st (G)	2nd (G)	1st (lb)	2nd (lb)
Hover		0	-	0	-	1.00	-	15,400	-
Vertical Takeoff	1	.07	.05	-.05	.06	1.09	1.08	18,200	17,000
	2	.05	-	.03	-	1.10	-	17,200	-
	3	.05	-	.03	-	1.11	-	17,500	-
	4	.04	-	.06	-	1.17	-	17,750	-
	5	.07	-	.02	-	1.12	-	17,700	-
	6	.01	-	0		1.11	-	17,800	-
Symmmetrical Dive and Pullout	1	.34	-.08	-.21	-.17	1.48	1.47	20,000	20,000
	2	-.10	-.06	-.20	-.16	1.58	1.52	20,400	20,100
	3	-.11	-.14	-.20	-.12	1.64	1.56	21,000	20,500
	4	-.15	-.12	-.14	-.17	1.65	1.52	21,500	21,000
	5	-.14	-.02	-.11	-.21	1.56	1.50	19,950	19,750
	6	-.16	-.10	-.10	-.13	1.56	1.55	20,600	20,200
Roll Reversal	1	-.02	-.04	-.09	-.02	1.12	1.10	16,400	16,200
	2	-.05	-.07	0	-.04	1.10	1.08	17,300	16,000
	3	-.08	-.08	-.13	-.14	1.10	1.20	18,200	16,300
	4	-.06	-.09	-.09	-.19	1.13	1.32	17,000	18,400
	5	-.06	-	-.04	-	1.15	-	16,800	-
	6	-.12	-	-.15	-	1.24	-	19,200	-

TABLE 9. PEAK VALUES, CONFIGURATION IIB

Maneuver and Number		Aircraft Load Factor				Leg $T_{L_{max}}$ Tension								Cable Tension $T_{C_{max}}$	
		Long-tndl $N_{x_{max}}$ (G)	Lateral $N_{y_{max}}$ (G)	Vertical $N_{z_{max}}$		Aft Left		Aft Right		Fwd Left		Fwd Right			
				1st (G)	2nd (G)	1st (lb)	2nd (lb)	1st (lb)	2nd (lb)	1st (lb)	2nd (lb)	1st (lb)	2nd (lb)	1st (lb)	2nd (lb)
Hover	1	0	.01	1.00	-	3,900	-	5,100	-	5,500	-	3,800	-	17,350	-
Vertical Takeoff	1	.09	.06	1.25	1.15	5,250	4,900	6,800	5,800	6,700	6,400	5,600	5,050	24,000	21,000
	2	.01	.05	1.20	1.08	4,950	4,750	6,300	5,800	6,250	6,100	4,900	4,800	21,500	20,400
	3	.05	.05	1.21	1.15	5,200	4,800	6,400	6,300	6,400	6,150	4,900	5,050	21,900	21,300
	4	0	.02	1.15	1.08	4,750	4,850	6,300	6,250	6,200	6,250	5,250	4,750	21,200	20,400
	5	.01	.03	1.23	1.10	5,300	5,200	6,650	6,350	6,650	6,400	5,200	4,650	22,500	21,100
	6	.01	.01	1.15	1.10	4,900	4,700	6,350	6,150	6,350	6,100	4,900	4,650	21,500	20,250
Symmetrical Dive and Pullout	1	-.18	-.12	1.30	-	4,550	-	6,500	-	5,950	-	5,850	-	21,600	-
	2	-.05	.01	1.34	1.34	5,300	5,200	7,450	7,400	6,650	6,650	6,300	6,400	24,600	24,500
	3	-.19	-.11	1.24	1.28	4,500	4,500	6,700	6,800	5,800	5,700	5,850	5,850	21,700	21,800
	4	-.30	-.06	1.36	1.23	5,300	4,100	7,450	6,650	6,600	5,200	6,100	5,300	24,400	20,200
	5	-.21	-.11	1.27	1.21	5,150	4,450	7,100	6,550	6,300	5,800	5,850	5,700	23,400	21,600
	6	-.25	-.04	1.20	-	4,500	-	6,750	-	5,700	-	5,300	-	21,000	-
Roll Reversal	1	-.13	.01	1.03	1.09	3,900	4,100	6,000	6,300	5,000	5,200	5,150	5,400	18,900	19,400
	2	-.06	-.06	1.02	1.12	3,750	4,450	6,100	6,500	4,800	5,550	5,150	5,550	18,500	20,600
	3	-.14	.05	1.06	-	3,850	-	6,350	-	5,000	-	5,000	-	19,000	-
	4	-.03	0	1.04	-	4,000	-	6,200	-	5,100	-	5,100	-	19,200	-
	5	-.10	.07	1.07	-	4,800	-	5,200	-	6,350	-	3,800	-	19,000	-
	6	-.06	.07	1.13	-	4,900	-	5,450	-	6,600	-	4,200	-	20,100	-

TABLE 10. PEAK VALUES, CONFIGURATION II 4PT

Maneuver and Number		Aircraft Load Factor				Cable Tension $T_{C_{max}}$								Sum of Cable Tensions $\Sigma T_{C_{max}}$	
		Long-tdnl $N_{x_{max}}$ (G)	Lateral $N_{y_{max}}$ (G)	Vertical $N_{z_{max}}$ 1st (G)	Vertical $N_{z_{max}}$ 2nd (G)	Aft Left 1st (lb)	Aft Left 2nd (lb)	Aft Right 1st (lb)	Aft Right 2nd (lb)	Fwd Left 1st (lb)	Fwd Left 2nd (lb)	Fwd Right 1st (lb)	Fwd Right 2nd (lb)	1st (lb)	2nd (lb)
Hover	1	0	-.02	1.00	-	4,300	-	3,850	-	3,700	-	4,150	-	16,000	-
	2	0	-.04	1.01	-	4,450	-	3,850	-	3,350	-	4,300	-	15,950	-
Vertical Takeoff	1	.02	-.02	1.29	-	5,200	-	4,900	-	4,850	-	5,100	-	20,050	-
	2	.03	-.0	1.14	-	4,850	-	4,250	-	4,000	-	4,750	-	17,850	-
	3	.03	-.01	1.26	-	5,200	-	4,950	-	4,950	-	5,000	-	20,100	-
	4	.02	-.05	1.34	-	5,600	-	5,150	-	4,550	-	5,300	-	20,600	-
	5	0	-.07	1.35	-	5,650	-	4,850	-	4,450	-	5,600	-	20,550	-
	6	0	-.07	1.32	-	5,350	-	4,950	-	3,350	-	5,300	-	20,150	-
Symmetrical Dive and Pullout	1	.06	-.08	1.51	-	6,350	-	6,250	-	6,500	-	5,500	-	24,600	-
	2	0	-.07	1.48	1.54	6,350	6,700	5,850	6,200	6,150	6,200	5,700	5,850	24,050	24,950
	3	0	-.03	1.61	1.50	6,500	6,550	6,200	6,000	6,350	5,900	5,850	5,850	24,900	24,300
	4	0	-.07	1.61	1.52	6,400	6,650	6,400	6,250	6,700	6,150	5,700	5,850	25,200	24,900
	5	.05	-.09	1.47	1.49	6,300	6,450	6,200	6,300	6,250	6,250	5,650	5,700	24,400	24,700
	6	-.15	-.15	1.37	1.35	6,100	6,200	5,800	5,800	6,000	5,350	6,200	5,300	24,100	22,650
Roll Reversal	1	0	-.05	1.32	-	6,000	-	5,650	-	5,700	-	5,200	-	22,550	-
	2	0	-.12	1.14	1.45	6,150	6,150	4,900	6,200	5,100	5,850	4,950	5,300	21,100	23,500
	3	-.11	-.10	1.15	1.53	6,250	6,450	4,800	6,250	5,050	5,850	5,000	5,900	21,100	24,450
	4	-.04	-.10	1.16	1.51	6,150	6,400	4,850	6,300	4,900	6,050	5,050	5,650	20,950	24,400
	5	-.06	-.04	1.28	1.58	5,500	6,350	5,300	6,500	5,200	6,200	4,950	5,850	20,950	24,950
	6	0	-.11	1.23	1.48	5,950	6,100	5,150	6,000	5,300	5,850	5,500	5,500	21,450	23,450
	7	0	-.04	1.76	-	6,850	-	6,850	-	6,550	-	6,250	-	26,500	-

TABLE 11. PEAK VALUES, CONFIGURATION IIIB

Maneuver and Number		Aircraft Load Factor				Leg Tension $T_{L_{max}}$								Cable Tension $T_{C_{max}}$	
		Long-tdnl $N_{x_{max}}$ (G)	Lateral $N_{y_{max}}$ (G)	Vertical $N_{z_{max}}$		Aft	Left	Aft	Right	Fwd	Left	Fwd	Right		
				1st (G)	2nd (G)	1st (lb)	2nd (lb)	1st (lb)	2nd (lb)	1st (lb)	2nd (lb)	1st (lb)	2nd (lb)	1st (lb)	2nd (lb)
Hover	1	.07	.01	1.00	-	1,000	-	2,050	-	2,600	-	800	-	7,000	-
Vertical Takeoff	1	.08	.08	1.26	1.35	1,550	1,700	2,400	2,650	2,800	3,000	1,350	1,400	8,550	9,000
	2	.10	.12	1.30	-	1,400	-	2,500	-	2,950	-	1,350	-	8,900	-
	3	.10	.09	1.36	-	1,700	-	2,500	-	3,200	-	1,300	-	8,700	-
	4	.01	0	1.54	-	1,750	-	-	-	3,200	-	1,450	-	9,800	-
	5	.03	.01	1.57	-	1,750	-	-	-	3,300	-	1,800	-	10,000	-
	6	.05	.02	1.64	-	1,650	-	-	-	3,300	-	1,700	-	9,800	-
Symmetrical Dive and Pullout	1	-.06	-.05	1.40	-	1,400	-	2,250	-	2,750	-	1,200	-	8,200	-
	2	-.06	.01	1.47	-	1,400	-	2,300	-	2,800	-	1,300	-	8,250	-
	3	-.05	-.03	1.38	-	1,400	-	2,350	-	2,800	-	1,200	-	8,400	-
	4	-.10	-.05	1.45	-	1,500	-	2,400	-	2,950	-	1,300	-	8,400	-
	5	-.05	0	1.40	1.38	1,350	1,350	2,100	2,300	2,700	2,800	1,350	1,300	8,000	7,950
	6	-.09	-.13	1.38	1.47	1,300	1,400	2,250	2,300	2,600	2,800	1,100	1,250	7,600	8,200
Roll Reversal	1	-.10	-.06	1.06	-	1,200	-	1,750	-	2,400	-	1,050	-	6,700	-
	2	-.10	-.03	1.06	-	1,200	-	1,800	-	2,400	-	1,100	-	6,850	-
	3	-.11	-.07	1.07	1.06	1,150	1,250	1,700	1,850	2,300	2,400	850	1,000	6,400	6,700
	4	-.14	-.09	1.08	-	1,300	-	2,000	-	2,550	-	1,150	-	7,250	-
	5	-.09	-.09	1.09	-	1,250	-	1,850	-	2,400	-	1,000	-	6,900	-
	6	-.12	0	1.09	-	1,250	-	2,050	-	2,450	-	1,100	-	7,200	-

TABLE 12. PEAK VALUES, CONFIGURATION III 4PT

Maneuver and Number		Aircraft Load Factor				Cable Tension $T_{C_{max}}$								Sum of Cable Tensions $\Sigma T_{C_{max}}$	
		Long-tdnl $N_{x_{max}}$ (G)	Lateral $N_{y_{max}}$ (G)	Vertical $N_{z_{max}}$		Aft Left		Aft Right		Fwd Left		Fwd Right			
				1st (G)	2nd (G)	1st (lb)	2nd (lb)	1st (lb)	2nd (lb)	1st (lb)	2nd (lb)	1st (lb)	2nd (lb)	1st (lb)	2nd (lb)
Hover	1	0	0	1.00	-	1,200	-	850	-	1,000	-	1,200	-	4,250	-
	2	0	.05	1.04	-	1,300	-	750	-	850	-	1,100	-	4,000	-
Vertical Takeoff	1	.06	.02	1.30	1.34	1,800	1,900	1,600	1,475	1,550	1,600	1,750	1,725	6,700	6,700
	2	.05	0	1.32	1.33	1,700	1,700	1,300	1,400	1,225	1,400	1,600	1,500	5,825	6,000
	3	.06	.01	1.34	1.36	1,675	1,900	1,450	1,550	1,550	1,600	1,600	1,800	6,275	6,850
	4	.04	-.07	1.69	-	2,250	-	1,550	-	1,650	-	1,850	-	7,300	-
	5	.04	.02	1.57	-	2,250	-	1,450	-	1,600	-	1,850	-	7,150	-
	6	.05	-.04	1.66	-	2,450	-	1,650	-	1,800	-	2,000	-	7,900	-
Symmetrical Dive and Pullout	1	0	-.04	1.55	-	2,100	-	2,350	-	2,350	-	1,900	-	8,700	-
	2	0	-.02	1.65	-	2,300	-	2,550	-	2,550	-	2,050	-	9,450	-
	3	-.05	-.07	1.59	-	2,150	-	2,650	-	2,700	-	1,800	-	9,300	-
	4	-.14	-.09	1.47	1.59	1,450	2,150	2,050	2,300	2,400	2,600	1,500	1,950	7,400	9,000
	5	-.18	-.14	1.71	1.61	2,150	2,750	2,150	2,700	2,200	2,300	2,050	2,300	8,550	10,050
	6	-.14	-.15	1.50	1.58	2,450	2,250	1,800	2,000	1,850	1,750	2,250	2,150	8,350	8,150
Roll Reversal	1	-.04	-.06	1.44	1.36	1,900	1,750	2,200	1,900	2,350	2,000	1,500	1,400	7,950	7,050
	2	-.09	-.11	1.48	1.54	2,200	2,150	2,000	2,350	2,000	2,400	1,900	1,850	8,100	8,750
	3	-.06	-.06	1.32	1.64	1,650	2,000	2,000	2,350	2,100	2,550	1,250	1,700	7,000	8,600
	4	-.13	-.02	1.55	1.71	1,700	2,150	2,600	2,550	2,800	2,550	1,300	1,750	8,400	9,000
	5	-.08	-.10	1.33	1.62	1,800	2,000	1,600	2,400	1,750	2,600	1,750	1,700	6,900	8,700
	6	-.12	-.06	1.54	1.82	1,700	2,200	2,300	2,250	2,500	2,200	1,300	1,950	7,800	8,600
	7	-.01	-.09	2.16	-	2,600	-	2,500	-	2,350	-	2,550	-	10,000	-

TABLE 13. NONDIMENSIONALIZED DATA, CONFIGURATION IP

Maneuver and Number		Position of Peak	Aircraft Load Factor $N_{z_{max}}$ (G)	Cable Tension Load Factor $LFT_{C_{max}}$
Hover	1	-	1.00	1.026
Vertical Takeoff	1	1st	1.09	1.213*
	1	2	1.08	1.133
	2	1st	1.10	1.146
	3	1st	1.11	1.166
	4	1st	1.17	1.183
	5	1st	1.12	1.179
	6	1st	1.11	1.186
Symmetrical Dive and Pullout	1	1st	1.48	1.333
	1	2nd	1.47	1.333
	2	1st	1.58	1.359
	2	2nd	1.52	1.339
	3	1st	1.64	1.399
	3	2nd	1.56	1.366
	4	1st	1.65	1.433
	4	2nd	1.52	1.399
	5	1st	1.56	1.329
	5	2nd	1.50	1.316
	6	1st	1.56	1.373
	6	2nd	1.55	1.346
Roll Reversal	1	1st	1.12	1.093
	1	2nd	1.10	1.079
	2	1st	1.10	1.153
	2	2nd	1.08	1.066
	3	1st	1.10	1.074
	3	2nd	1.20	1.086
	4	1st	1.13	1.133
	4	2nd	1.32	1.226
	5	1st	1.15	1.119
	6	1st	1.24	1.279

*Highest ratio of Cable Tension Load Factor to Aircraft Load Factor = 1.11

TABLE 14. NONDIMENSIONALIZED DATA, CONFIGURATION IIB

Maneuver and Number		Position of Peak	Aircraft Load Factor $N_{z_{max}}$ (G)	Leg Tension Load Factor $LFT_{L_{max}}$ *** Aft Left	Aft Right	Fwd Left	Fwd Right	Cable Tension Load Factor $LFT_{C_{max}}$
Hover	1	1st	1.00	.789	1.032	1.113	.769	1.095
Vertical Takeoff	1	1st	1.25	1.063	1.317	1.356	1.134	1.515**
	1	2nd	1.15	.992	1.174	1.296	1.022	1.325
	2	1st	1.20	1.002	1.275	1.265	.992	1.357
	2	2nd	1.08	.961	1.174	1.235	.972	1.288
	3	1st	1.21	1.053	1.296	1.296	.992	1.382
	3	2nd	1.15	.972	1.275	1.245	1.022	1.344
	4	1st	1.15	.961	1.275	1.255	1.063	1.338
	4	2nd	1.08	.982	1.265	1.265	.961	1.288
	5	1st	1.23	1.073	1.346	1.346	1.053	1.420
	5	2nd	1.10	1.053	1.285	1.296	.941	1.332
	6	1st	1.15	.992	1.285	1.285	.992	1.357
	6	2nd	1.10	.951	1.245	1.235	.941	1.278
Symmetrical Dive and Pullout	1	1st	1.30	.921	1.316	1.204	1.184	1.363
	2	1st	1.34	1.073	1.508	1.346	1.275	1.553
	2	2nd	1.34	1.053	1.498	1.346	1.296	1.546
	3	1st	1.28	.921	1.356	1.174	1.184	1.370
	3	2nd	1.28	.911	1.377	1.154	1.184	1.376
	4	1st	1.36	1.073	1.508	1.336	1.235	1.540
	4	2nd	1.23	.830	1.346	1.053	1.073	1.275
	5	1st	1.27	1.042	1.437	1.275	1.184	1.477
	5	2nd	1.21	.901	1.326	1.174	1.154	1.363
	6	1st	1.20	.911	1.366	1.154	1.073	1.325
Roll Reversal	1	1st	1.03	.789	1.215	1.012	1.042	1.193
	1	2nd	1.09	.830	1.275	1.053	1.093	1.224
	2	1st	1.02	.759	1.235	.972	1.042	1.168
	2	2nd	1.12	.901	1.316	1.123	1.123	1.300
	3	1st	1.06	.779	1.285*	1.012	1.012	1.199
	4	1st	1.04	.810	1.255	1.042	1.032	1.212
	5	1st	1.07	.972	1.053	1.285	.769	1.199
	6	1st	1.13	.992	1.103	1.336	.850	1.269

*Highest ratio of Leg Tension Load Factor to Aircraft Load Factor = 1.21
**Highest ratio of Cable Tension Load Factor to Aircraft Load Factor= 1.21
***Highest value in each set of Leg Tension Load Factors is underlined.

TABLE 15. NONDIMENSIONALIZED DATA, CONFIGURATION II 4PT

Maneuver and Number		Position of Peak	Aircraft Load Factor $N_{z_{max}}$ (G)	Cable Tension Load Factor $LFT_{C_{max}}$ ** Aft Left	Aft Right	Fwd Left	Fwd Right
Hover	1	-	1.00	1.109	.993	.955	1.071
Hover	1	-	1.01	1.148	.993	.864	1.109
Vertical Takeoff	1	1st	1.29	1.342	1.264	1.251	1.316
	2	1st	1.14	1.251	1.097	1.032	1.226
	3	1st	1.26	1.342	1.277	1.277	1.290
	4	1st	1.34	1.445	1.329	1.174	1.368
	5	1st	1.35	1.458	1.251	1.148	1.445
	6	1st	1.32	1.381	1.277	1.174	1.368
Symmetrical Dive and Pullout	1	1st	1.51	1.639	1.613	1.677	1.419
	2	1st	1.48	1.639	1.510	1.587	1.471
	2	2nd	1.54	1.729	1.600	1.600	1.510
	3	1st	1.61	1.677	1.600	1.639	1.510
	3	2nd	1.50	1.690	1.548	1.522	1.510
	4	1st	1.61	1.652	1.652	1.729	1.471
	4	2nd	1.52	1.716	1.613	1.587	1.510
	5	1st	1.47	1.626	1.600	1.613	1.458
	5	2nd	1.49	1.664	1.626	1.613	1.471
	6	1st	1.37	1.574	1.497	1.548	1.600
	6	2nd	1.35	1.600	1.497	1.381	1.368
Roll Reversal	1	1st	1.32	1.548	1.458	1.471	1.342
	2	1st	1.14	1.587	1.264	1.316	1.277
	2	2nd	1.45	1.587	1.600	1.510	1.368
	3	1st	1.15	1.613*	1.239	1.303	1.290
	3	2nd	1.53	1.664	1.613	1.510	1.522
	4	1st	1.16	1.587	1.251	1.264	1.303
	4	2nd	1.51	1.652	1.626	1.561	1.458
	5	1st	1.28	1.419	1.368	1.342	1.277
	5	2nd	1.58	1.639	1.690	1.600	1.510
	6	1st	1.23	1.535	1.329	1.368	1.303
	6	2nd	1.48	1.574	1.548	1.510	1.419
	7	1st	1.76	1.768	1.768	1.690	1.613

*Highest ratio of Cable Tension Load Factor to Aircraft Load Factor = 1.40

**Highest value in each set of Leg Tension Load Factors is underlined

TABLE 16. NONDIMENSIONALIZED DATA, CONFIGURATION IIIB

Maneuver and Number	Position of Peak	Aircraft Load Factor $N_{z_{max}}$ (G)	Leg Tension Load Factor $LFT_{L_{max}}$ *** Aft Left	Aft Right	Fwd Left	Fwd Right	Cable Tension Load Factor $LFT_{C_{max}}$
Hover 1	-	1.00	.574	1.177	1.493	.459	1.254
Vertical Takeoff 1	1st	1.26	.890	1.378	<u>1.608</u>	.775	1.531
Vertical Takeoff 1	2nd	1.35	.976	1.522	<u>1.723</u>	.804	1.612
Vertical Takeoff 2	1st	1.30	.804	1.435	<u>1.694</u>	.775	1.594**
Vertical Takeoff 3	1st	1.36	.976	1.435	<u>1.838</u>	.746	1.558
Vertical Takeoff 4	1st	1.54	1.005	1.751	<u>1.838</u>	.832	1.755
Vertical Takeoff 5	1st	1.57	1.005	1.809	<u>1.895</u>	1.033	1.791
Vertical Takeoff 6	1st	1.64	.947	1.838	<u>1.895</u>	.976	1.755
Symmetrical Dive and Pullout 1	1st	1.40	.804	1.292	<u>1.579</u>	.689	1.469
Symmetrical Dive and Pullout 2	1st	1.47	.804	1.321	<u>1.608</u>	.746	1.477
Symmetrical Dive and Pullout 3	1st	1.38	.804	1.349	<u>1.608</u>	.689	1.504
Symmetrical Dive and Pullout 4	1st	1.45	.861	1.378	<u>1.694</u>	.746	1.504
Symmetrical Dive and Pullout 5	1st	1.40	.775	1.206	<u>1.550</u>	.775	1.433
Symmetrical Dive and Pullout 5	2nd	1.38	.775	1.321	<u>1.608</u>	.746	1.424
Symmetrical Dive and Pullout 6	1st	1.38	.746	1.292	<u>1.493</u>	.631	1.361
Symmetrical Dive and Pullout 6	2nd	1.47	.804	1.321	<u>1.608</u>	.717	1.469
Roll Reversal 1	1st	1.06	.689	1.005	<u>1.378</u>	.603	1.200
Roll Reversal 2	1st	1.06	.689	1.033	<u>1.378</u>	.631	1.227
Roll Reversal 3	1st	1.07	.660	.976	<u>1.321</u>	.488	1.147
Roll Reversal 3	2nd	1.06	.717	1.062	<u>1.378</u>	.574	1.200
Roll Reversal 4	1st	1.08	.746	1.148	<u>1.464</u>*	.660	1.298
Roll Reversal 5	1st	1.09	.717	1.062	<u>1.378</u>	.574	1.236
Roll Reversal 6	1st	1.09	.717	1.177	<u>1.407</u>	.631	1.289

*Highest ratio of Leg Tension Load Factor to Aircraft Load Factor = 1.36
**Highest ratio of Cable Tension Load Factor to Aircraft Load Factor=1.23
***Highest value in each set of Leg Tension Load Factors is underlined.

TABLE 17. NONDIMENSIONALIZED DATA, CONFIGURATION III 4PT

Maneuver and Number		Position of Peak	Aircraft Load Factor $N_{z_{max}}$ (G)	Cable Tension Load Factor $LFT_{C_{max}}$ ** Aft Left	Aft Right	Fwd Left	Fwd Right
Hover	1	-	1.00	1.004	.711	.836	1.004
Hover	2	-	1.04	1.087	.627	.711	.920
Vertical Takeoff	1	1	1.30	1.506	1.338	1.297	1.464
	1	2	1.34	1.589	1.234	1.338	1.443
	2	1	1.32	1.422	1.087	1.025	1.338
	2	2	1.33	1.422	1.171	1.171	1.255
	3	1	1.34	1.401	1.213	1.297	1.338
	3	2	1.36	1.589	1.297	1.338	1.506
	4	1	1.69	1.882	1.297	1.380	1.548
	5	1	1.57	1.882	1.213	1.338	1.548
	6	1	1.66	2.050	1.380	1.506	1.673
Symmetrical Dive and Pullout	1	1	1.55	1.757	1.966	1.966	1.589
	2	1	1.65	1.924	2.133	2.133	1.715
	3	1	1.59	1.799	1.217	2.259	1.506
	4	1	1.47	1.213	1.715	2.008	1.255
	4	2	1.59	1.799	1.924	2.175	1.631
	5	1	1.71	1.799	1.799	1.841	1.715
	5	2	1.61	2.301	2.259	1.924	1.924
	6	1	1.50	2.050	1.506	1.548	1.882
	6	2	1.58	1.882	1.673	1.464	1.799
Roll Reversal	1	1	1.44	1.589	1.841	1.996	1.255
	1	2	1.36	1.464	1.589	1.673	1.171
	2	1	1.48	1.841	1.673	1.673	1.589
	2	2	1.54	1.799	1.966	2.008	1.548
	3	1	1.32	1.380	1.673	1.757	1.046
	3	2	1.64	1.673	1.966	2.133	1.422
	4	1	1.55	1.422	2.175	2.343*	1.087
	4	2	1.71	1.799	2.133	2.133	1.464
	5	1	1.33	1.506	1.338	1.464	1.464
	5	2	1.62	1.673	2.008	2.175	1.422
	6	1	1.54	1.422	1.924	2.092	1.087
	6	2	1.82	1.841	1.882	1.841	1.631
	7	1	2.16	2.175	2.092	1.966	2.133

*Highest ratio of Cable Tension Load Factor to Aircraft Load Factor = 1.51

**Highest value in each set of Leg Tension Load Factors is underlined

For Configuration III 4PT, the maximum individual load leveller cable readings were divided by the static tension in each cable. The latter value was derived by calculating the true angle of a cable to the vertical and resolving the static weight of the empty container, i.e., 4,590 pounds, along four such cables. From the geometry of the configuration the cable angle was found to be 16° 16', so the static tension in each of the four cables becomes 4,590/4 sec 16° 16', i.e., 1,195 pounds.

LOAD FACTOR PLOTS AND ANALYTICAL PROCESSING

The tensions, in load factor form, were then plotted against aircraft load factor for each of the five configurations, resulting in the following graphs:

Figure 17 for Configuration IP cable

Figure 19 for Configuration IIB cable

Figure 21 for Configuration IIB legs

Figure 23 for Configuration II 4PT cables

Figure 24 for Configuration IIIB cable

Figure 25 for Configuration IIIB legs

Figure 26 for Configuration III 4PT cables

Figure 27 is an explanatory graph, used to depict the key to the test point symbols and lines (and also to illustrate the analytical process described later). The maneuvers are represented by the same symbols as used in Reference 1, i.e.,

triangle = vertical takeoff (VTO)

circle = symmetrical dive and pullout (SDPO)

square = roll reversal (RR)

Owing to the congestion of test points on Figures 17, 19 and 21, portions of these plots were rescaled for clarity (at a factor of X5) as shown in Figures 18, 20 and 22 respectively. Where multiple legs or cables are involved, as in Figures 21, 22, 23, 25 and 26, only the highest of each set of four tension load factors was plotted, i.e., the values shown underlined in Tables 14, 15, 16 and 17 respectively. The lower tensions shown in the remaining legs are of no interest.

The two-dimensional distribution of points on these plots was analyzed with the aid of a Monroe 1860 (Statistical) Programmable Calculator to determine correlation coefficient, slope, intercept and standard error. These were derived from the following expressions [5].

5. Leabo, Dick A., BASIC STATISTICS, Homewood, Ill., Richard D. Irwin, Inc., March 1972.

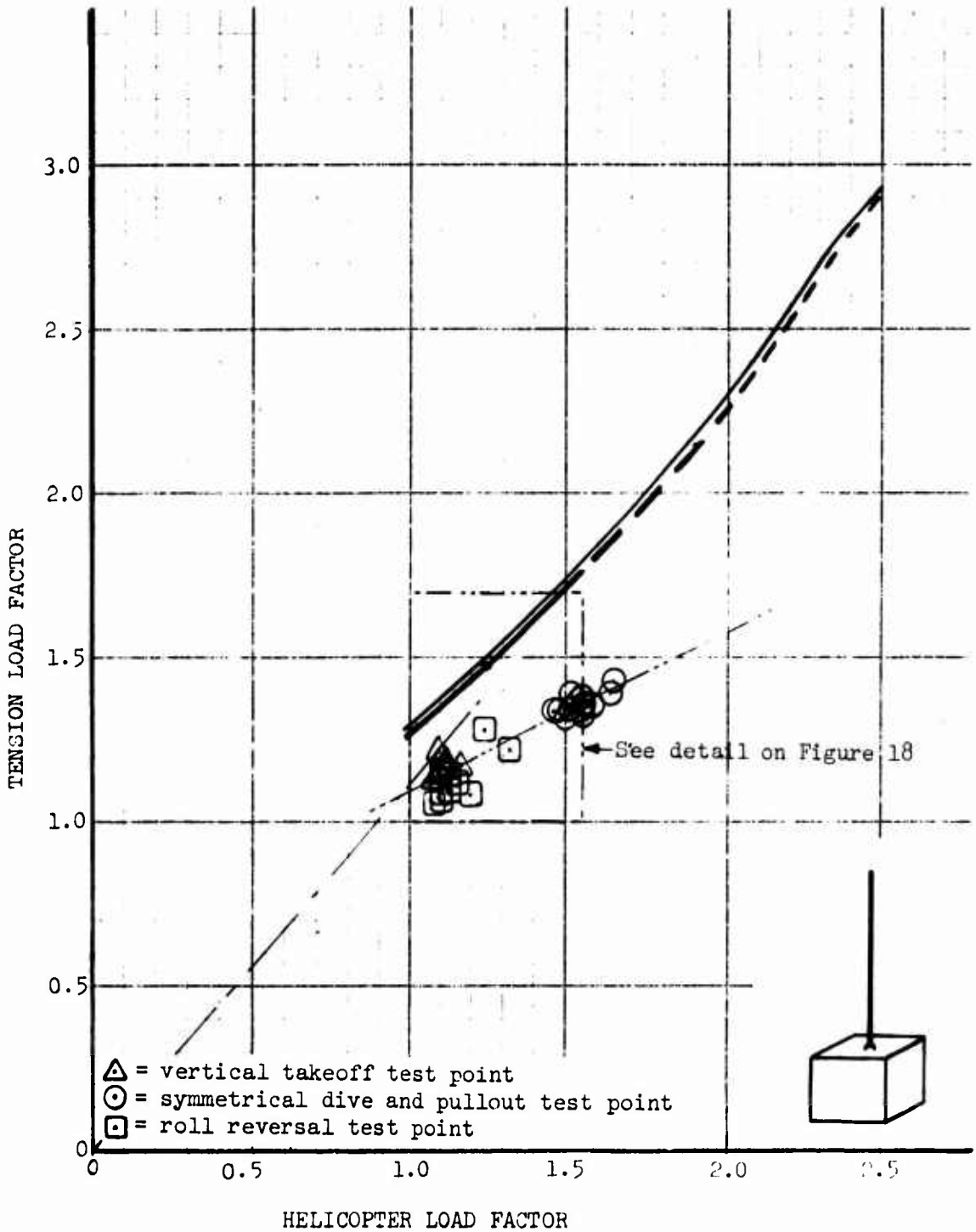

Figure 17. Tension Load Factor Versus Helicopter Load Factor, Configuration IP Cable.

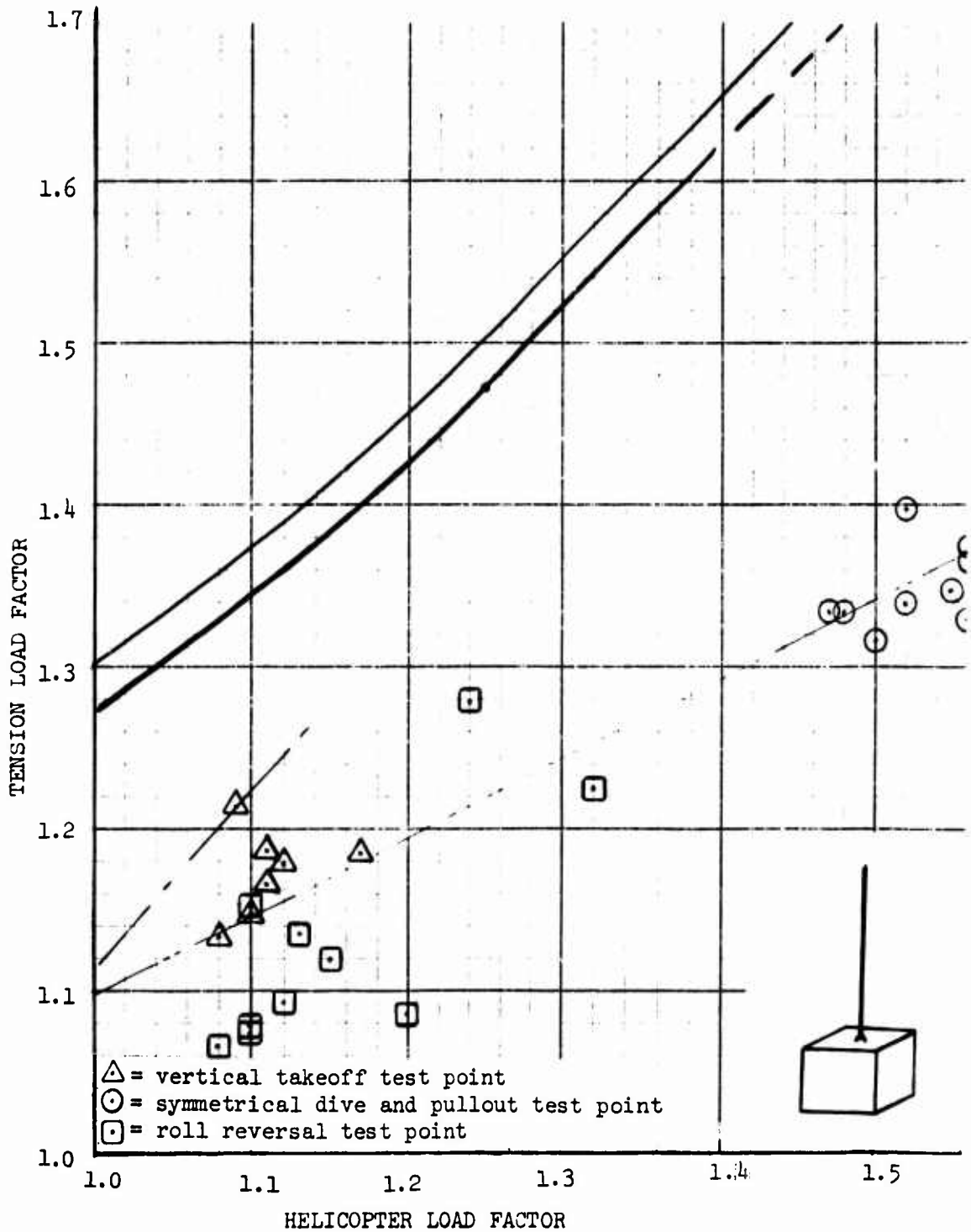

Figure 18. Tension Load Factor Versus Helicopter Load Factor, Configuration IP Cable (Figure 17 detail).

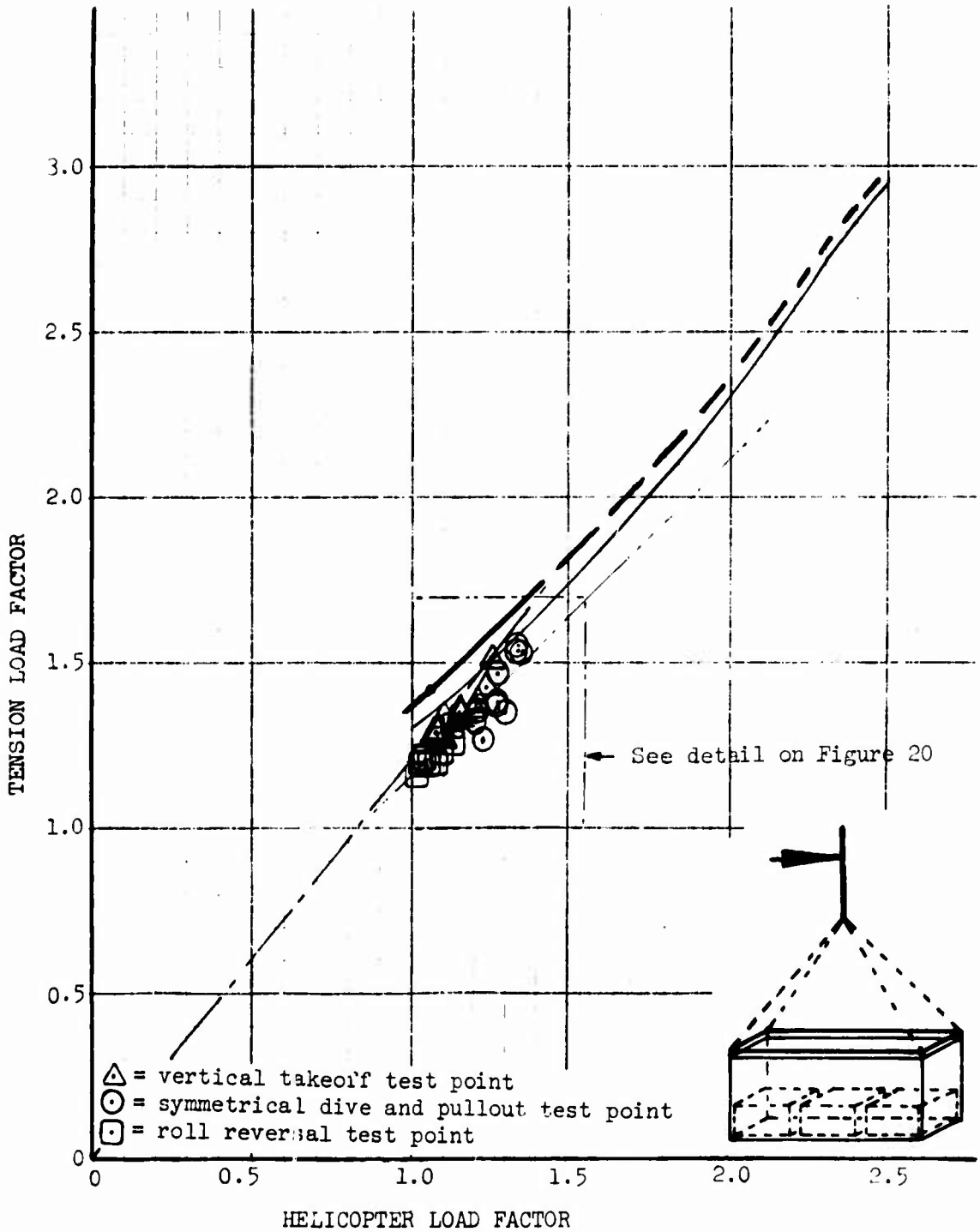

Figure 19. Tension Load Factor Versus Helicopter Load Factor, Configuration IIB Cable.

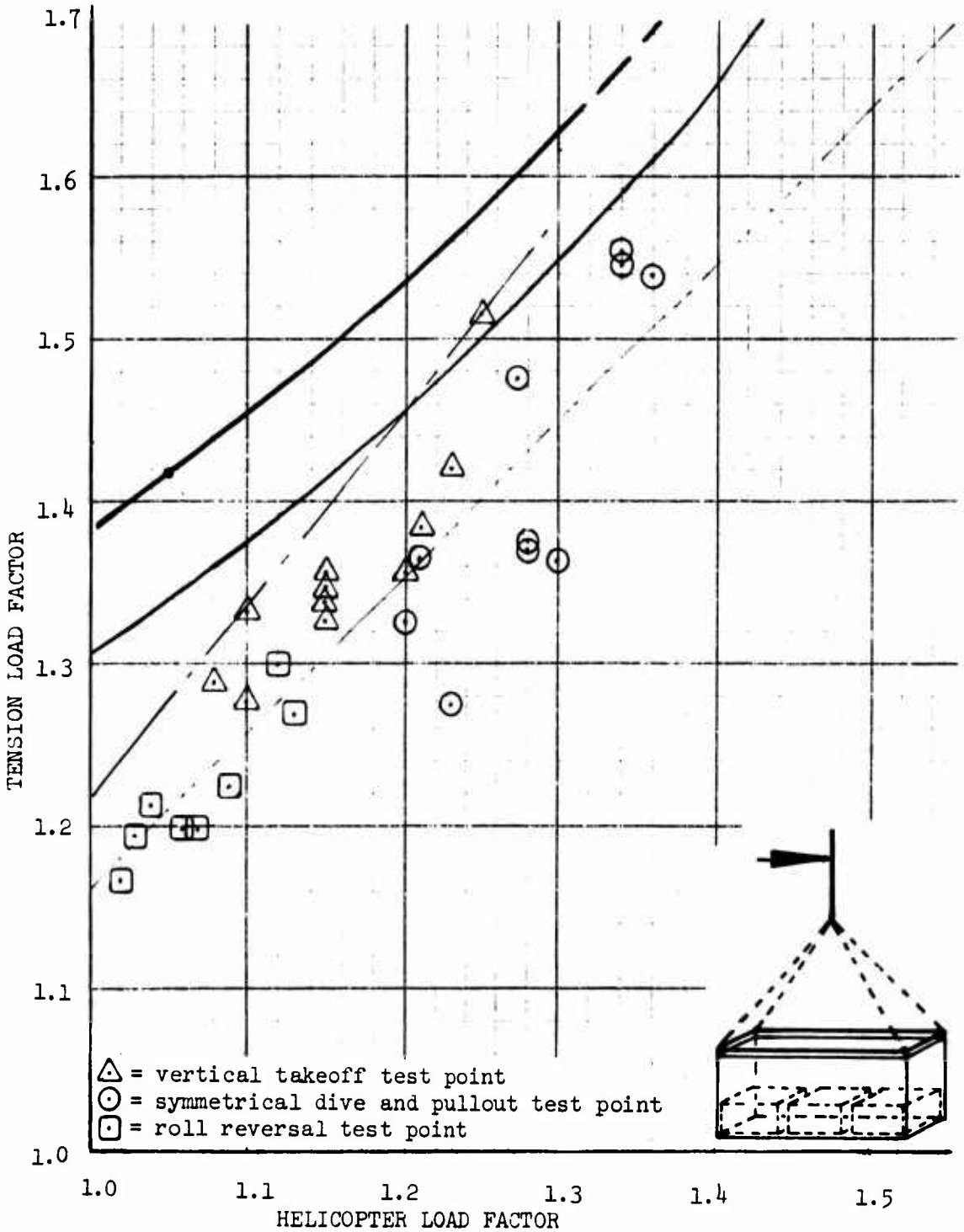

Figure 20. Tension Load Factor Versus Helicopter Load Factor, Configuration IIB Cable (Figure 19 detail).

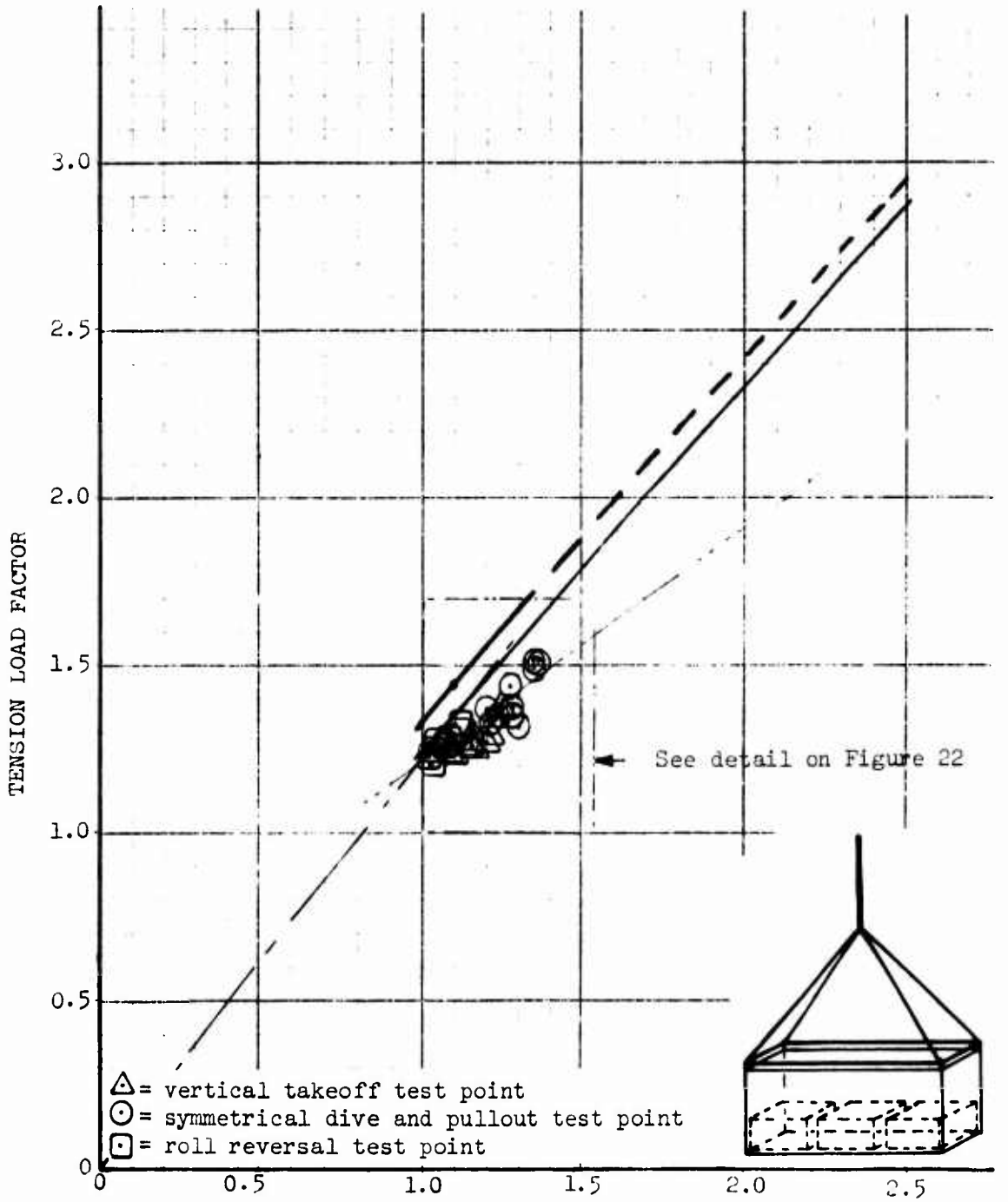

Figure 21. Tension Load Factor Versus Helicopter Load Factor, Configuration IIB Legs.

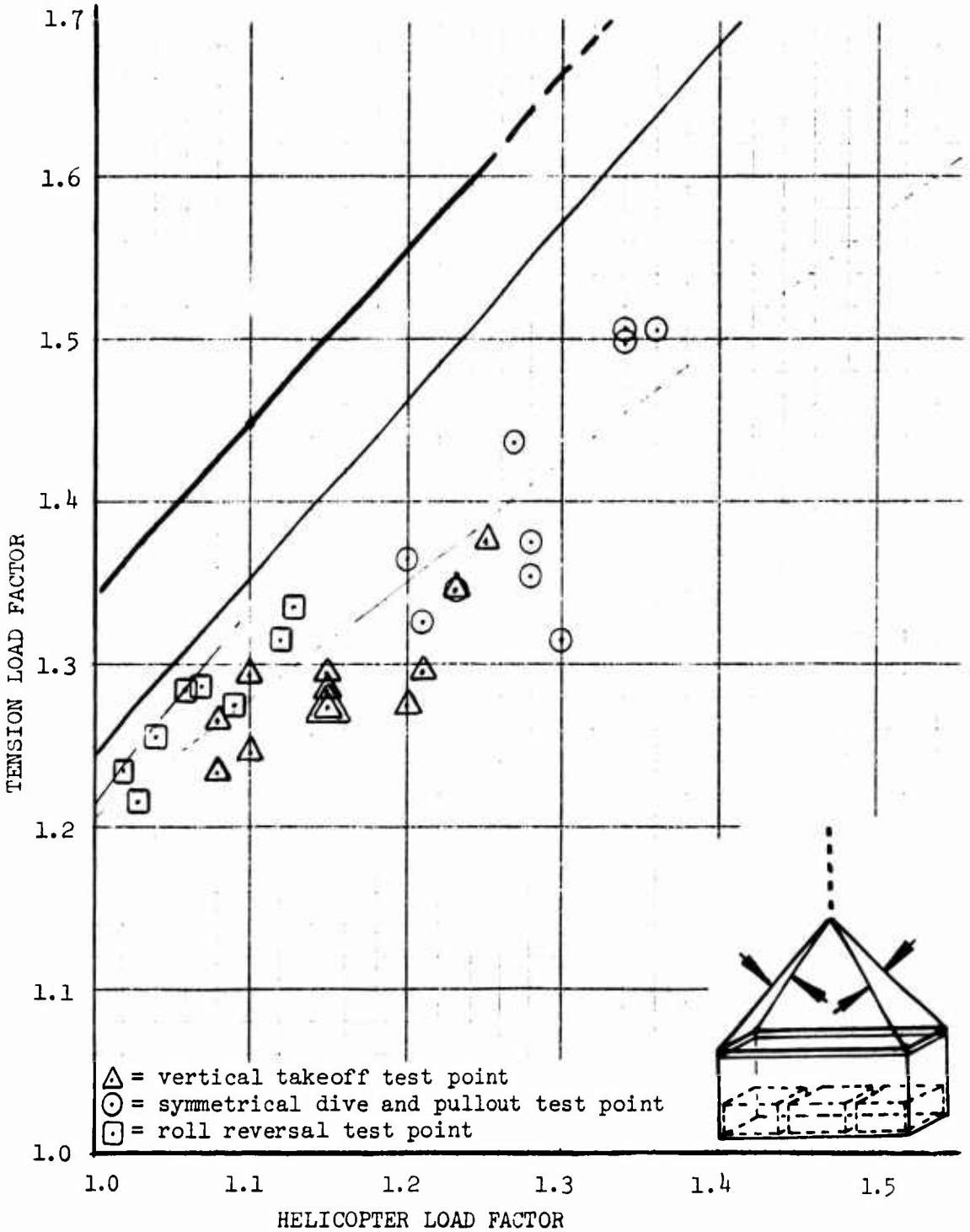

Figure 22. Tension Load Factor Versus Helicopter Load Factor, Configuration IIB Legs (Figure 21 detail).

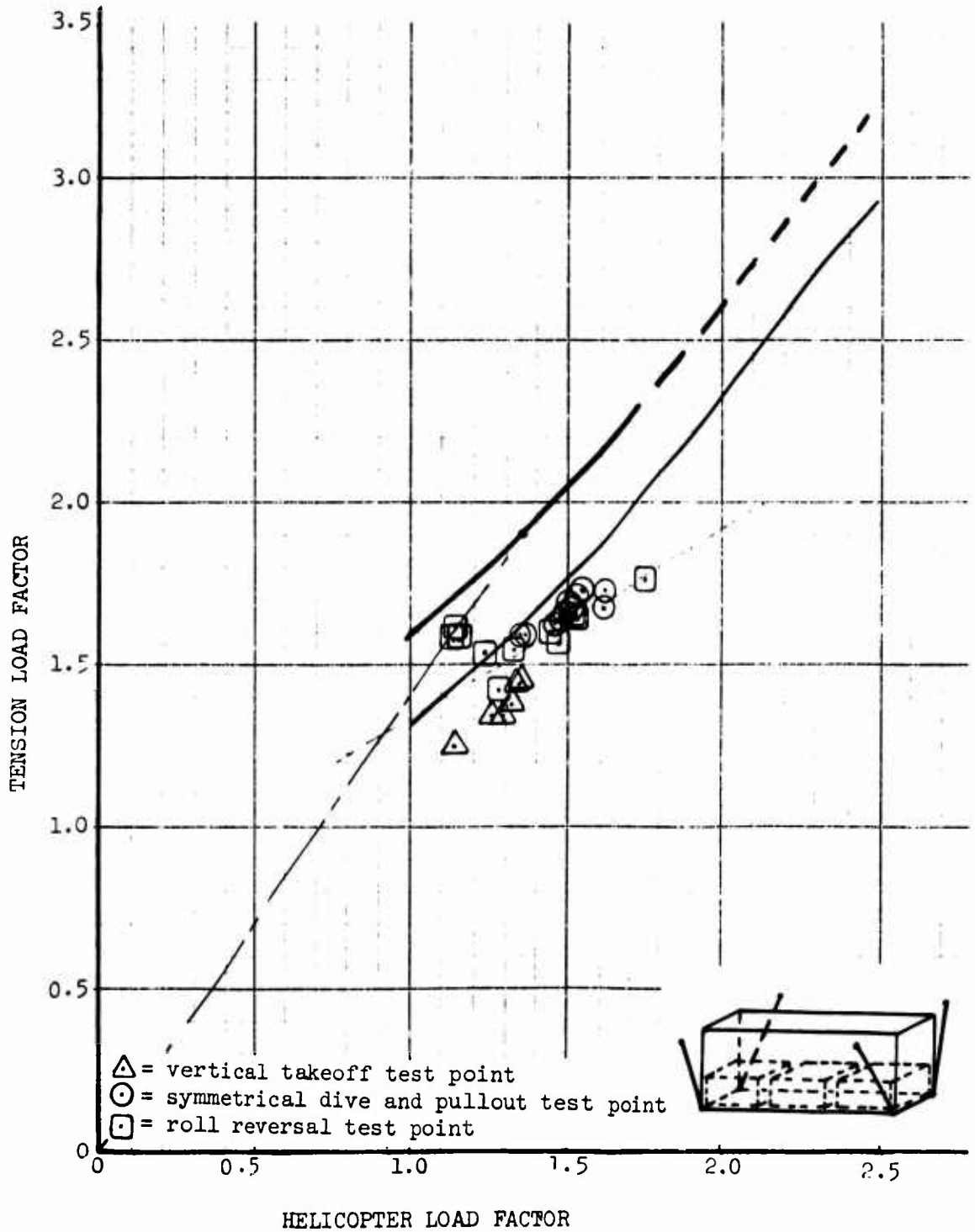

Figure 23. Tension Load Factor Versus Helicopter Load Factor, Configuration II 4PT Cables.

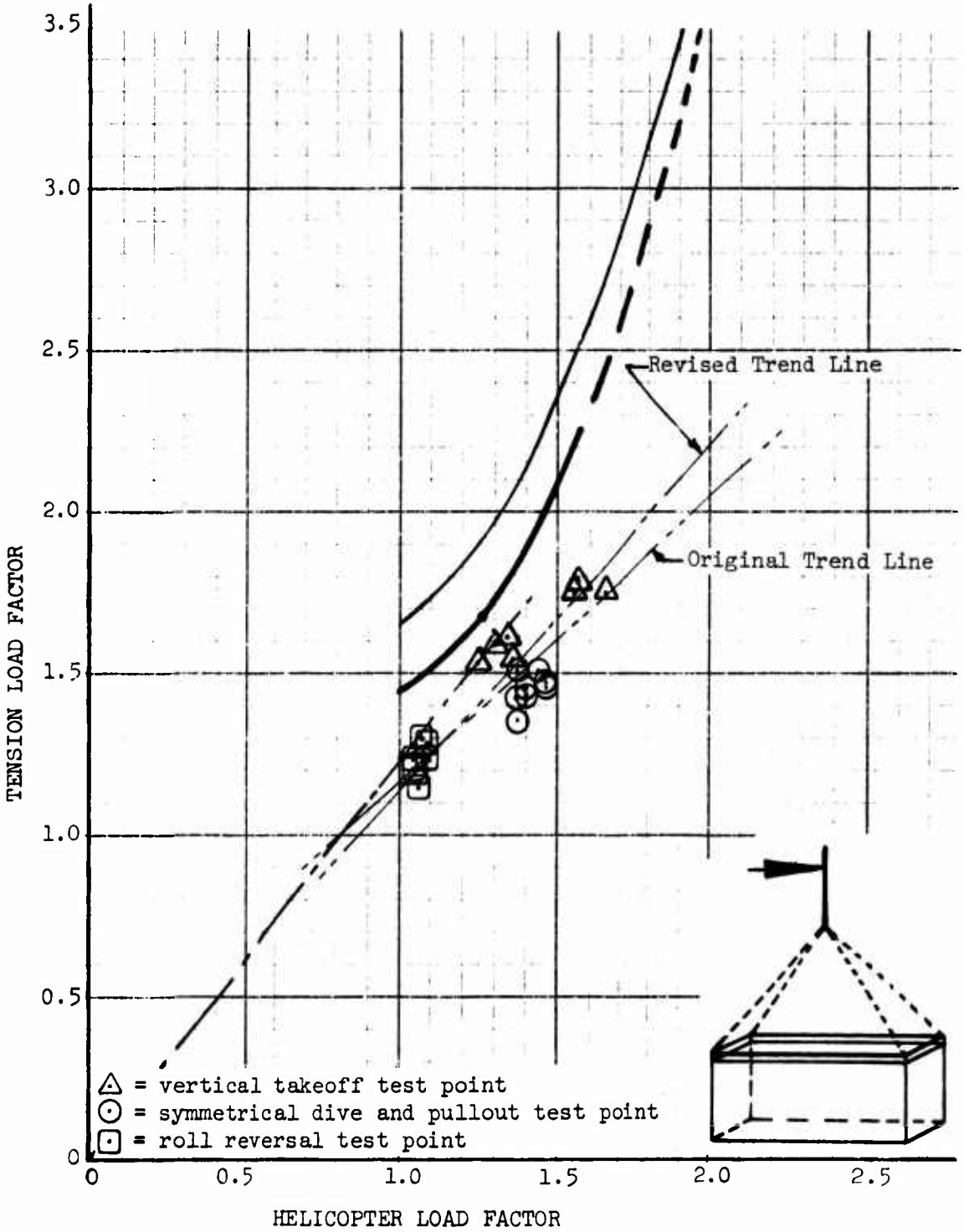

Figure 24. Tension Load Factor Versus Helicopter Load Factor, Configuration IIIB Cable.

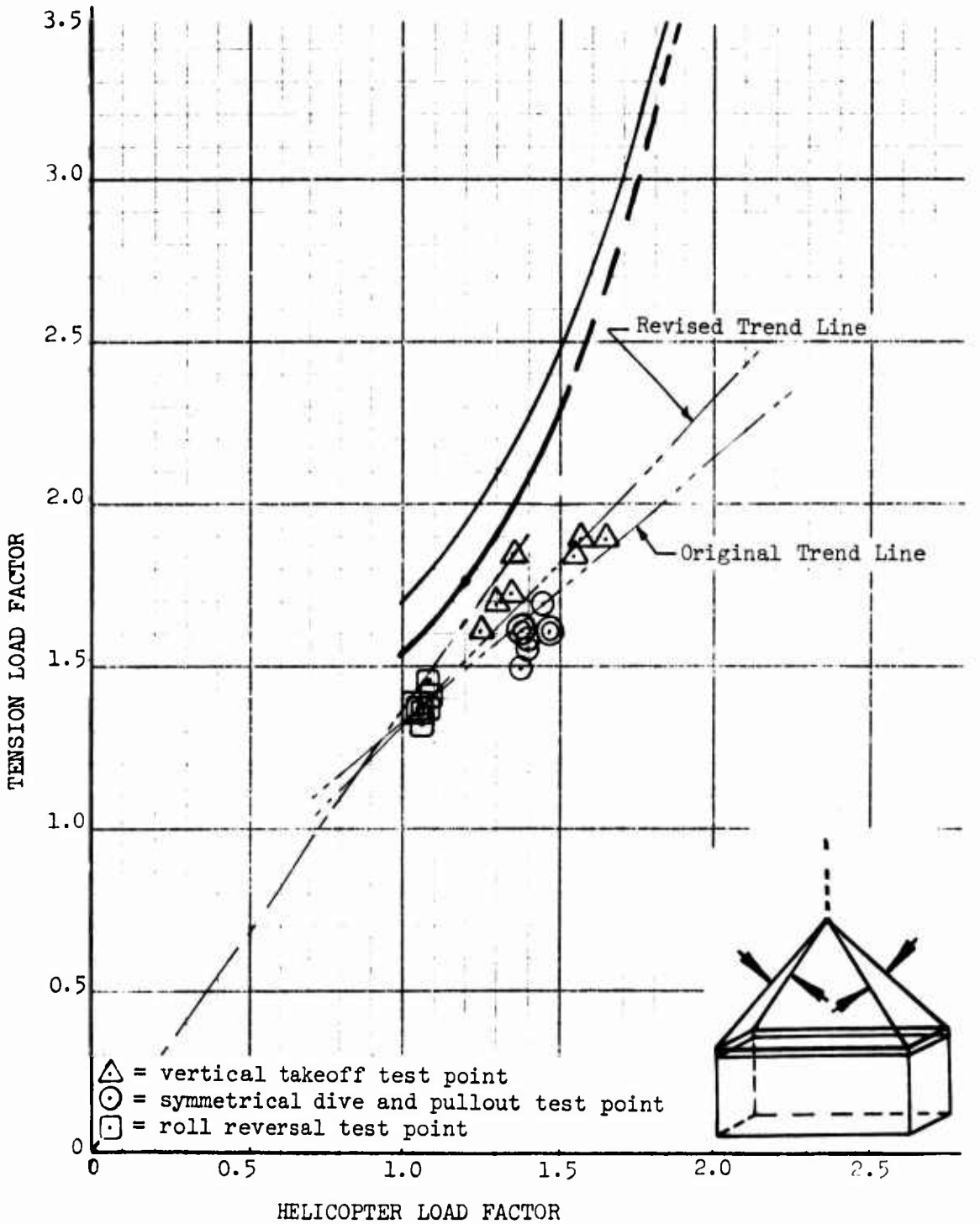

Figure 25. Tension Load Factor Versus Helicopter Load Factor, Configuration IIIB Legs.

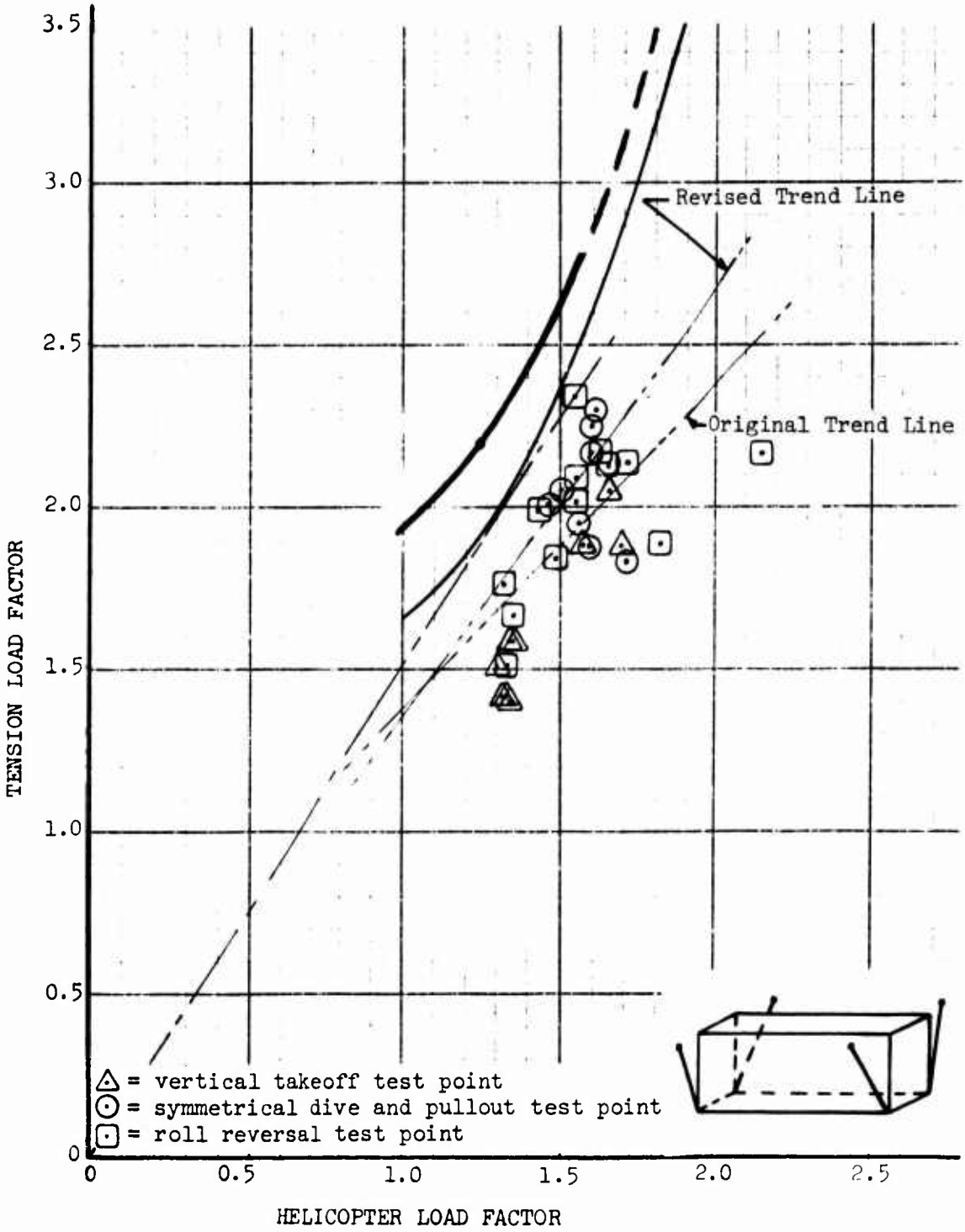

Figure 26. Tension Load Factor Versus Helicopter Load Factor, Configuration III 4PT Cables.

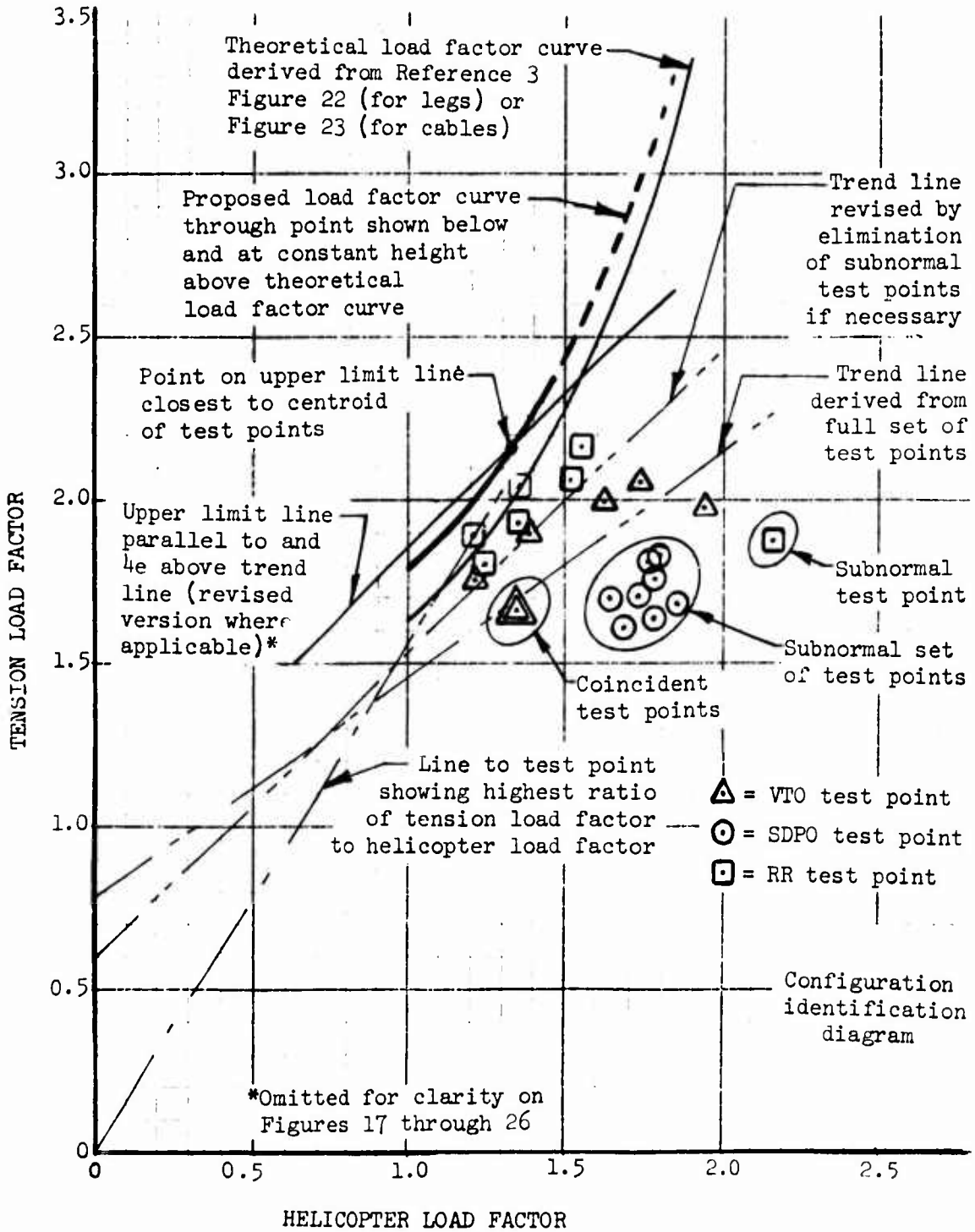

Figure 27. Tension Load Factor Versus Helicopter Load Factor, Key Diagram for Figures 17 through 26.

$$LR = \frac{\Sigma XY - \frac{\Sigma X \Sigma Y}{N}}{\sqrt{\left(\Sigma X^2 - \frac{(\Sigma X)^2}{N}\right)\left(\Sigma Y^2 - \frac{(\Sigma Y)^2}{N}\right)}} \quad (1)$$

$$S = \frac{\Sigma XY - \frac{\Sigma X \Sigma Y}{N}}{\Sigma X^2 - \frac{(\Sigma X)^2}{N}} \quad (2)$$

$$I = \frac{\Sigma Y - S\Sigma X}{N} \quad (3)$$

$$e = \sqrt{\frac{\Sigma (Y - Y_c)^2}{N-2}} \quad (4)$$

where

e = standard error of estimate (or standard deviation)
I = intercept
LR = correlation coefficient
N = number of test points
S = slope
X = abscissa (i.e., aircraft load factor)
Y = ordinate (i.e., tension load factor)
Y_c = expected value of Y

In the expression for e (Equation 4), the denominator N-2 is used in place of the customary N, because two pairs of coordinates are prerequisite to the establishment of a regression. Hence, two degrees of freedom are lost, and the count begins normally when N is 3.

LR is a measure of the degree of conformity of the plotted test points (its use will be explained later), S and I permit the trend line for the set of test points to be plotted (S being the gradient of the trend line and I being its position on the vertical axis), and e expresses the plot distribution (measured vertically, not normally, on either side of the trend line). Table 18 summarizes the above statistical parameters for the seven plots, and the resultant trend lines are shown on Figures 17 through 26.

Table 18 also records the highest ratio of tension load factor to aircraft load factor for each plot. As demonstrated on Figure 27 the test point producing this highest ratio is that which is at maximum elevation from the origin. In some cases (e.g., on Figures 19 and 21) it is difficult to identify the relevant test point (even when the plot is magnified), but the type of maneuver is readily apparent. In other cases (e.g., on Figures 24 and 25), two types of maneuvers are close candidates for maximum load factor augmentation. Calculation of the ratio will of course

TABLE 18. STATISTICAL SUMMARY

Configuration	Table No.	Figure No.	Correlation Coefficient LR	Slope S	Intercept I	Standard Error e	Highest Ratio of Load Factor		Highest Tension Load Factor	
							Value	** Maneuver	Value	** Maneuver
IP	13	17	.856	.485	.614	.062	1.11	VTO No. 1	1.433	SDPO No. 4
IIB Cable	14	19	.890	.963	.209	.050	1.22	VTO No. 1	1.553	SDPO No. 2
IIB Legs	14	21	.866	.690	.513	.040	1.22	RR No. 3	1.508	SDPO No. 2
II 4PT	15	23	.710	.583	.759	.095	1.40	RR No. 3	1.768	RR No. 7
IIIB Cable	16	24	.876	.884	.287	.093	1.23	VTO No. 2	1.791	VTO No. 5
IIIB Cable*	16	24	.967	1.080	.090	.063	1.23	VTO No. 2	1.791	VTO No. 5
IIIB Legs	16	25	.867	.824	.507	.091	1.36	RR No. 4	1.895	VTO No. 6
IIIB Legs*	16	25	.963	1.008	.324	.062	1.36	RR No. 4	1.895	VTO No. 6
III 4PT	17	26	.659	.993	.379	.211	1.51	RR No. 4	2.343	RR No. 4
III 4PT*	17	26	.727	1.320	.017	.128	1.51	RR No. 4	2.343	RR No. 4

*Revised after elimination of subnormal test points.
**All occurred on first peak.

resolve the doubtful cases but is valid only within the limits of experimental accuracy; hence, both maneuvers should be considered equal in this respect. It is useful to examine the relationship between configuration and highest load factor ratio to determine whether any pattern is evident. This is reviewed later (see page 61).

DERIVATION OF NEW PROPOSED LOAD FACTOR CURVES

Filtering out low values was taken a stage further in the following manner. Where it was obvious from the plots that the test points associated with a particular type of maneuver were well below the trend line, such points were eliminated from further consideration. For example, from Figure 25 it was evident that symmetrical dives and pullouts (represented by circles) induced a less significant load factor augmentation than the other maneuvers and were therefore irrelevant in an investigation of leg load maximums for Configuration IIIB (though they are, of course, perfectly valid test points). Also, certain individual test points were discarded if they were significantly isolated below the trend line. Thus in Figure 26, three roll reversal test points and one symmetrical dive and pullout test point were judged to be so subnormal that their inclusion in the analysis produced an unwarranted optimization of the trend line.

Three plots were subjected to the above filtering process, namely, Figures 24, 25 and 26, and the statistical analyses for the retained test points were rerun to produce the revised values shown in Table 18. It will be seen that the correlation coefficients have increased by approximately 10%, indicating an improvement in the validity of the analysis. Note, however, that the correlation coefficients of the unfiltered plots are not particularly high (especially that for Configuration II 4PT, Figure 23), due to some exceptionally high test points which must obviously be retained in a valid search for maximums. Revised trend lines were constructed on Figures 24, 25 and 26, using the same line designation, but they can be identified by the fact that they are obviously steeper.

Statistical theory predicts that, with a normal distribution, 99.994% of all possible test points will fall within a band of width equal to four times the standard error on either side of the trend line. To represent the upper boundary of this distribution zone, a line can be drawn parallel to and at a distance of 4e vertically, not normally, above the trend line (or revised trend line where applicable) as illustrated on Figure 27. On this line, a point was selected that lay closest to the estimated centroid of the test points. (It was not necessary to compute the centroid position since the subsequent process was geometrically noncritical; in other words, a minor inaccuracy in the estimation would have negligible effect.) Through this point a line was drawn at a constant vertical distance from the simulated load factor curve given in Reference 3. This line is the proposed load factor curve to replace the simulated curve. On each plot it is shown by a heavy line, broken as it progresses beyond the test points to reflect the lack of substantiating data in the upper regions.

The processes depicted on Figure 27 were applied to Figures 17 through 26, but to avoid confusion the upper limit line was erased after it had served

its purpose as an aid to positioning the proposed load factor curve.

In the following section the significance of each graph and the validity of its associated test points are discussed.

DISCUSSION OF RESULTS

A search for comparable features in the plots indicates that they can be considered to fall into three groups as follows:

Configurations IP, IIB cable and IIB legs (Figures 17, 19, and 21)

Configurations IIIB cable and IIIB legs (Figures 24, 25)

Configurations II 4PT and III 4PT cables (Figures 23, 26)

They will therefore be discussed initially as groups, followed by a general discussion of the whole set.

Configurations, IP, IIB Cable and IIB Legs

No subnormal test points are evident on Figures 17, 19, or 21; in fact, the density of distribution necessitated replotting to a larger scale (Figures 18, 20 and 22). SDPO appears to generate higher absolute load factors but lower load factor ratios than VTO and RR. This is particularly noticeable on Figure 17 and may be attributable to vertical drag characteristics. Highest load factor ratios were generated by VTO for IP and IIB cable and by RR for IIB legs, but by a narrow margin. The proposed load factor curves for IP and IIB cable conform very closely to the simulated curve, falling slightly below and above, respectively. The proposed load factor curve for IIB legs is also slightly above the simulated curve. The trend line slopes for the IP cable and IIB legs are distinctly less than the gradient of any part of the simulated curves so it is probable that at the higher levels the load factor augmentation is less than anticipated.

Configurations IIIB Cable and IIIB Legs

The SDPO test point clusters were clearly subnormal on both Figures 24 and 25. The trend lines were therefore recalculated with all these eliminated. VTO generates higher absolute load factor than RR, probably due to the effect of downwash on the large empty container, but load factor ratios are very consistent. Highest load factor ratios were generated by VTO, but by a very narrow margin. The proposed load factor curves for IIIB cable and IIIB legs are distinctly lower than the simulated curves. The trend line slopes conform quite closely to the gradient of the simulated curves in the test point region.

Configurations II 4PT and III 4PT Cables

A wide scattering of test points is evident. The VTO test point clusters were slightly subnormal on Figure 26; also three RR test points and one SDPO test point were considered subnormal. The trend line was therefore

recalculated with all those eliminated. There is an unusually high group of RR test points on Figure 23 (well above the simulated curve) and these were of course retained. RR and SDPO are about equally responsible for high absolute load factor values, but load factor ratios are definitely higher for RR. The low absolute values and ratios associated with VTO may be due to the minimal effect of downwash on the closely attached container. The proposed load factor curves for II 4PT and III 4PT cables are substantially higher than the simulated curve. The trend line slopes conform fairly closely to the gradient of the simulated curves in the test point region.

All Configurations

The degree of validity of Figures 22 and 23 of Reference 3 can now be assessed by comparing them with the proposed load factor curves of the relevant configurations.

The Type I and II curve on Figure 22 of Reference 3 applies to Figures 17/18, 19/20 and 23. For Figures 17/18 and 19/20, extremely close agreement to the simulated curve is evident. The very slight elevation of the proposed curve for IIB cable is of no great consequence. For Figure 23 however, the discrepancy is large, and the appearance of four test points clearly above the simulated curve (a peculiarity of this configuration alone) indicates that the applicability of the curve is less valid here than in the other configurations.

The Type III curve on Figure 22 of Reference 3 applies to Figures 24 and 26. The curve can be regarded as conservative for the IIIB cable, but it is sufficiently far below the proposed curve for the III 4PT cables to warrant reconsideration of the applicability of the curve to this configuration. Although all the test points were under the simulated curve, they were widely scattered, resulting in a large standard error.

The Type I and II curve on Figure 23 of Reference 3 applies to Figure 21/22 only. Close agreement to the simulated curve is evident, and although the proposed curve is slightly higher (like the cable curve for this configuration shown on Figure 19/20), the trend line slope suggests that the simulated curve is conservative.

The Type III curve on Figure 23 of Reference 3 applies to Figure 25 only. The curve can be regarded as conservative (like the cable curve for this configuration shown on Figure 24, to which it shows remarkable affinity even in the distribution of test points).

Load Factor Augmentation

Table 18 recorded the highest ratio of leg or cable tension load factor to aircraft load factor for each configuration, and also the maneuvers responsible for these maximums. No consistent relationship between configurations and maneuvers was evident. Figure 28 presents the same information in a more graphic form. It shows, for all configurations, the maneuvers producing the highest tension load factors (in legs or cables) and the

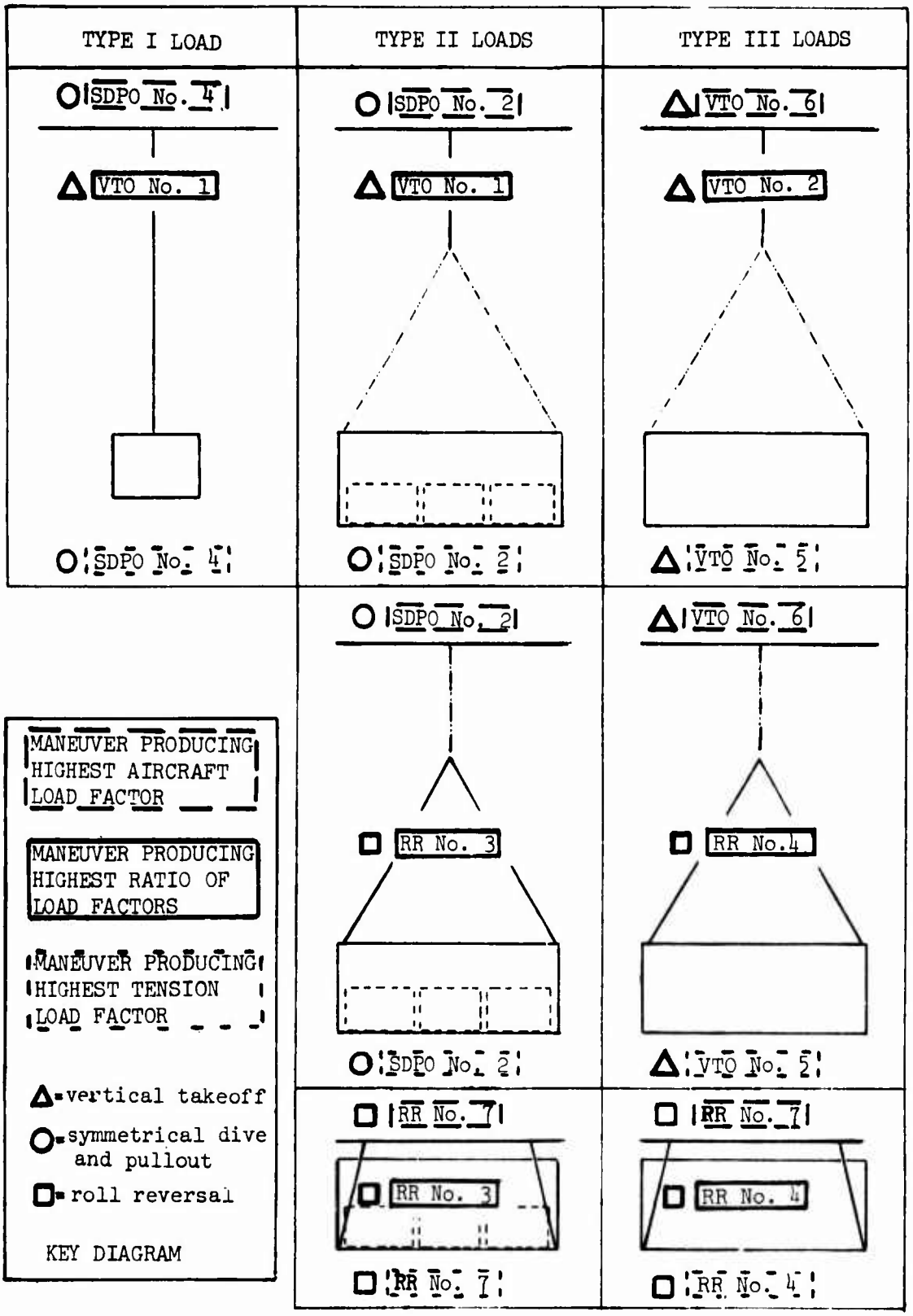

Figure 28. Analysis of Most Critical Manuevers.

highest aircraft load factors, as well as the highest ratios of these two parameters. A nebulous pattern begins to emerge, and it can be best summarized by the following statements:

1. Highest tension load factors and aircraft load factors are produced by: -

   SDPO for dense loads suspended via one point

   VTO for non-dense loads suspended via one point

   RR for dense and non-dense loads suspended via four points

   (The expression "via one point" covers not only Configuration IP but also Configurations IIB and IIIB, since the four legs of the slings converge to one apex fitting. The expression "via four points" covers Configuration II 4PT and III 4PT, self-evidently.)

2. Highest ratios of tension load factors to aircraft load factors are produced by: -

   VTO for dense and non-dense loads on single tension members.

   RR for dense and non-dense loads on multiple tension members.

   (The expression "on single tension members" covers the cables of Configurations IP, IIB and IIIB. The expressions "on multiple tension members" covers the legs of Configurations IIB and IIIB, and the cables of Configurations II 4PT and III 4PT.

Examination of the numerical basis for the above statements (See Tables 13 through 17) will show that they are valid by a rather unsubstantial margin. There is no sound basis to suggest that one maneuver is significantly worse than another. The simulator study conclusion that symmetrical dive and pullout is the most critical maneuver is partially supported by the evidence of Figures 17/18, 19/20, 21/22 and 23 (configurations with dense loads) but not Figures 24, 25 and 26 (configurations with non-dense loads).

CONCLUSIONS AND RECOMMENDATIONS

Compared with the tension load factor/helicopter load factor relationships established by the simulator study, the flight test results show that:

1. The simulator study produced essentially valid data for Configurations IB, IIB cables and IIB legs. This indicates that substantially correct criteria were used for the 25K and 60K slings, for these were based on the load factors derived for Type I and Type II load curves as explained on page 64 of Reference 4.

2. The simulator study produced ultraconservative data for Configurations IIIB cable and IIIB legs. This indicates that conservative criteria were used for the 6K slings, for these were based on the load factors derived for Type III load curves as explained on page 63 of Reference 4.

3. The simulator study produced optimistic data for Configurations II 4PT and III 4PT. However, the four-point/four-cable suspension is a system peculiar to the CH-54, and instead of slings it uses integral hoist cables which normally pull the load tight into the aircraft fuselage. In the flight tests, a slight gap was allowed between the container and the aircraft in order to approach the simulator study conditions. This may account for the higher load factors recorded by the flight tests.

Every effort was made to maximize the load readings and the interpretation of data. Thus, the pilot endeavoured to apply the highest possible dynamic loads, only peak values on the oscillograph records were extracted, the most loaded cable or leg in multiple tension member configurations was selected, and data which yielded test points well below the trend line were omitted from the statistical analysis. Hence, there can be a good level of confidence in the validity of the results in the flight regimes tested. However, it was rarely possible to achieve a helicopter load factor exceeding 2G, so the proposed load factor curves can only be tentatively extended beyond the test point regions. It is well established that in any program that supplies measured loads, the latter are usually well below the required design loads. It is emphasized that the tension load factors obtained in Reference 1 are essentially design requirement values.

It is recommended that the design requirements for the 25K sling (and hence the 20K pendant) and 60K sling be confirmed, but that the design requirements for the 6K sling (and hence the 6K pendant) be reduced by about 33% if the requirement for Type III loads is deleted. The 6K strength requirement was predicated on a worst-case load exemplified by an empty container on the UH-1 at 3.0 g. Since there are no other Type III loads currently in the inventory, and since the empty container weighs considerably less than 6,000 pounds, the 6K sling and pendant are seen to be overdesigned by about 33% for the vast majority of loads that they will cover.

Since the completion of the cargo sling development program there has been sufficient progress in advanced sling materials (such as the PRD-49-III mentioned on page 31 of Reference 4) to justify a reaxamination for sling

applications of any such materials and constructions for which the basic research has been completed.

REFERENCES

1. Briczinski, S. J., and Karas, G.R., CRITERIA FOR EXTERNALLY SUSPENDED HELICOPTER LOADS, Sikorsky Aircraft, Division of United Aircraft Corporation; USAAMRDL Technical Report 71-61, Eustis Directorate, U.S. Army Air Mobility Research and Development Laboratory, Fort Eustis, Virginia, November 1971, AD 740072.

2. Gustafson, Arthur J., Jr., Bryan, Max E., McIlwean, Edgar H., and Birocco, Eugene A., EFFECTS OF HELICOPTER EXTERNAL LOADS ON SLING PROPERTIES; USAAMRDL Technical Report 73-91, Eustis Directorate, U.S. Army Air Mobility Research and Development Laboratory, Fort Eustis, Virginia, September 1973, AD 774267.

3. Huebner, Walter E., DESIGN GUIDE FOR LOAD SUSPENSION POINTS, SLINGS, AND AIRCRAFT HARD POINTS, Sikorsky Aircraft, Division of United Aircraft Corporation; USAAMRDL Technical Report 72-36, Eustis Directorate, U.S. Army Air Mobility Research and Development Laboratory, Fort Eustis, Virginia, July 1972, AD 747814.

4. Hone, Horace T., Huebner, Walter E., and Baxter, Donald J., DEVELOPMENT OF CARGO SLINGS WITH NONDESTRUCTIVE CHECKOUT SYSTEMS, Sikorsky Aircraft, Division of United Aircraft Corporation; USAAMRDL Technical Report 73-106, Eustis Directorate, U.S. Army Air Mobility Research and Development Laboratory, Fort Eustis, Virginia, February 1974, AD 777497.

5. Leabo, Dick A., BASIC STATISTICS, Homewood, Ill., Richard D. Irwin, Inc., March 1972.

APPENDIX

DEVELOPMENT OF SLING DESIGN CRITERIA - AN OVERVIEW

The scientific development of sling design criteria was begun as a result of a meeting held at Fort Eustis in 1968. Attending were Army test agencies, Army sling user organizations, major helicopter manufacturers, sling manufacturers, and Army R&D personnel. The questions of how to rate a sling in terms of payload capability, and how to evaluate the remaining payload capability of a used sling were discussed, with no answers, for two days. The meeting did result in a positive plan for development of much-needed design criteria, not only for slings, but for aircraft hard points and for load suspension points. It was recognized that two basic kinds of information were needed:

1. What are the actual dynamic loads, caused by helicopter maneuvers in combination with aerodynamic gusts and buffeting, that are imposed on the load attachment points, the sling legs, and the aircraft hook?

2. How much loss in strength occurs over a period of one to two years in sling legs because of the detrimental effects of environment on sling leg materials?

The strength loss question was answered by USAAMRDL Tech Report 73-91, Effects of Helicopter External Loads on Sling Properties. Quantitative data on the deterioration of various textile webbings due to exposure to sunlight and various liquids, temperature, sand and dust, and fatigue were obtained by testing many samples. This program was conducted by the Eustis Directorate.

Concurrently, Sikorsky Aircraft performed Contract DAAJ02-70-C-0021, Criteria for Externally Suspended Helicopter Loads. The purpose of this program was to establish dynamic flight load factors in answer to question 1 above. This was accomplished through the use of a computerized flight simulator program coupled with the equations of motions of the slung load. The helicopter/slung load systems were flown through a series of flight maneuvers. Dynamic sling leg forces were compared with the corresponding static sling leg forces to obtain load factors. These load factors were compared with the accelerations of the aircraft C.G. for the maneuver. The flight simulator work was done using equations of motion for the CH-54 and the slung load. The resulting load factor curves were later extrapolated for other aircraft designed for performing flight maneuvers at higher or lower design load factors. The work of this program is discussed more fully in this report.

The dynamic load factors established as a result of this program, and the environmental degradation data were used by Sikorsky to prepare Design Guide for Load Suspension Points, Slings and Aircraft Hardpoints, USAAMRDL Technical Report 72-36. For each of the three design categories (load suspension points, slings, aircraft hardpoints) a design procedure was outlined. The design procedure outlined specific geometry and configu-

ration requirements so that vehicles and equipment would be compatible with slings, and so that slings would be compatible with aircraft hard points, all designed to the given requirements. In addition, strength requirements were given. The strength criteria were derived from the criteria obtained in the flight simulator program and then further modified as necessary to account for environmental degradation, depending on the sling material chosen. Graphs were included to show the maximum dynamic load likely to be encountered as a result of the flight maneuver load and the effect of aerodynamic gusts in combination. The curves on these graphs were plotted for aircraft having design flight load factors of from 1 to 3.

An aircraft with a design flight load factor of 3 is capable of performing a given maneuver more violently than another aircraft with a design flight load factor of 2. It is recognized that an aircraft with a given design flight load factor will not normally be capable of fully reaching this flight regime because of the softness of the rotor system. However, the curves do show the maximum anticipated dynamic load in a sling leg as a result of combining the aircraft's actual maneuver load capability with outside aerodynamic effects. The abscissa (aircraft load factor) provides a convenient index for comparing and locating aircraft by performance. Two curves are shown. In Type III loads (large surface area to weight ratio) the effects of aerodynamic gusts are proportionally more significant than on dense loads, and therefore the total sling leg load factor is higher.

Formulas for required sling leg strength given in USAAMRDL Technical Report 72-36 have been simplified for use by commercial operators in the U.S. The simplification removes the requirement to consult the sling leg tension factor curve and is applicable to Type I and Type II loads only. These formulas appear in the American National Standard for Rotorcraft External Loads, ANSI B30.12, and are repeated below.

Symbols: n = Design flight load factor for the rotorcraft (See the Rotorcraft Flight Manual)

W = Rated capacity of the entire sling

S = Service break strength of each leg

Pendant (one-legged sling): $S = 1.75nW$

For a two-legged sling: $S = 1.32nW$

For a three-legged sling: $S = 0.9nW$

For a four-legged sling: $S = 0.7nW$

The service break strength (S) is the actual break strength of the sling leg after one year of service. Reduced ultimate strength factors of TR 72-36 apply.

In 1974, the present program, Flight Load Investigation of Helicopter External Payloads, was undertaken to verify the work of the computer simulator program and to validate the strength criteria of Technical Report 72-36. This report fully describes the work of the program. The data points obtained are actual flight loads measured by instrumentation aboard a CH-54 aircraft with Sikorsky pilots flying the same external loads used in the simulator study.

The following types of instrumentation were used:

1. An eighteen channel light beam type recording oscillograph, Type 114, manufactured by Consolidated Electrodynamic Corporation.

2. Single axis piezoresistive low G (± 25) Type 2262 accelerometers, manufactured by Endevco.

3. A main load cell of 50,000 pound capacity, Baldwin-Lima Hamilton, Type U-1.

4. Individual sling leg load cells of 10,000 pound capacity, Baldwin-Lima Hamilton, Type U3G2.

Maneuvers were executed in a controlled manner and with severity always consistent with safety. All flights, except vertical takeoffs, were carried out at altitudes equivalent to densities of 2,000 ft. and airspeeds ranging from 35 to 92 knots indicated airspeed.

The scatter of points in many thousands of flight maneuvers will obviously be larger than the scatter obtained from six maneuvers of each type, and a statistical correction has been applied to account for this. The statistically corrected data is in close agreement with the strength criteria given in Technical Report 72-36.

LIST OF SYMBOLS

σ	standard error of estimate
I	intercept
LFT_C	cable tension load factor
LFT_L	leg tension load factor
LR	correlation coefficient
N	number of test points
N_x	helicopter longitudinal load factor
$N_{x_{max}}$	helicopter longitudinal load factor maximum
N_y	helicopter lateral load factor
$N_{y_{max}}$	helicopter lateral load factor maximum
N_z	helicopter vertical load factor
$N_{z_{max}}$	helicopter vertical load factor maximum
S	slope
$T_{C_{max}}$	maximum cable tension, lb
T_{C_S}	cable tension static trim value, lb
T_i	cable tension, lb
T_j	leg tension, lb
$T_{L_{max}}$	maximum leg tension, lb
T_{L_S}	leg tension static trim value, lb
X	abscissa
Y	ordinate
Y_c	expected value of Y